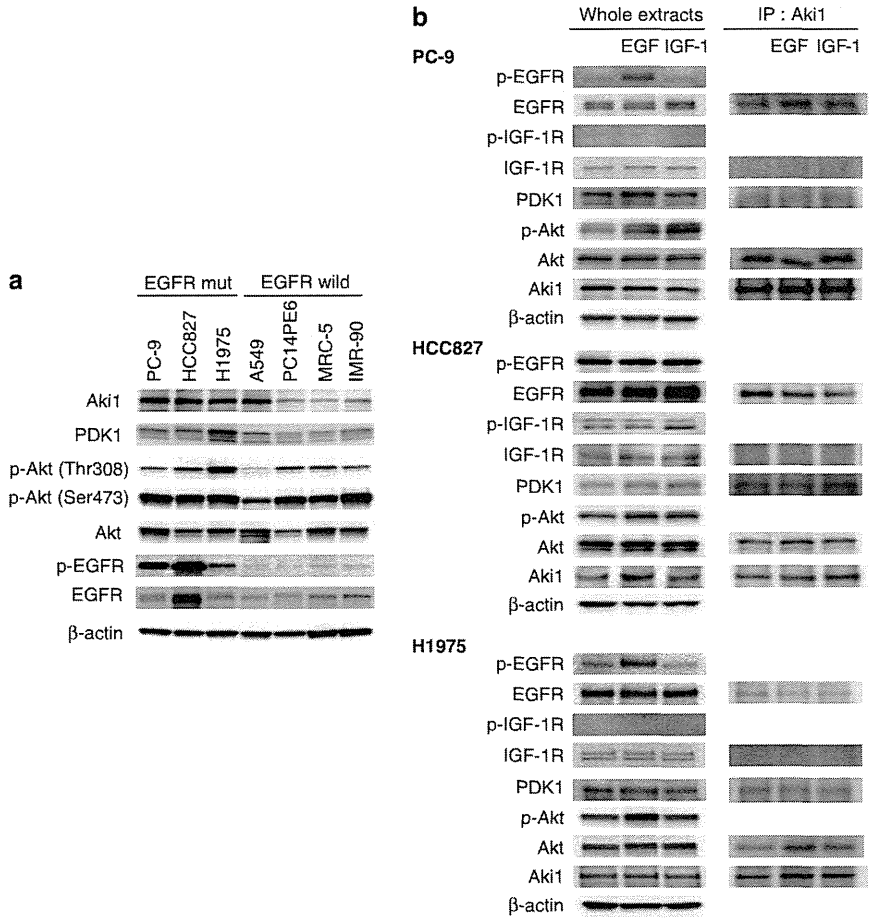

Figure 1. Aki1 expression and association to EGFR in EGFR mutant human lung cancer cell lines. (**a**) *EGFR* mutant human lung cancer cell lines (PC-9, HCC827 and H1975), *EGFR* wild-type human lung cancer cell lines (A549 and PC14PE6) and human lung fibroblast cell lines (MRC-5 and IMR-90) were lysed and the indicated proteins were detected by western blotting. (**b**) *EGFR* mutant lung cancer cell lines were treated with or without EGF (50 ng/ml) or IGF-1 (50 ng/ml) for 10 min. Then, cells were lysed and the indicated proteins were detected by western blotting with or without immunoprecipitation of Aki1.

knockdown decreased the levels of Akt and S6 phosphorylation, and increased the level of Par-4 and cleaved PARP, when combined with WZ4002 (Figure 5b). These results suggest the usefulness of *Aki1* knockdown combined with new generation EGFR-TKIs against lung cancer with *EGFR* T790M gatekeeper mutation.

Aki1 is frequently expressed in *EGFR* mutant lung cancer

We next examined Aki1 expression in 56 clinical specimens obtained from 56 lung cancer patients with *EGFR* mutation (Figure 6a and Supplementary Table S1). To confirm the specificity of the Aki1 by immunohistochemical staining, we performed Aki1 antibody absorption test by Aki1 peptide. The staining of Aki1 was remarkably diminished by pretreatment of sections with an Aki peptide at 4 °C overnight, compared with saline treatment, indicating the specificity of the antibody which we used for Aki1 staining (Supplementary Figure S6). Forty-two tumors were obtained from EGFR-TKI naive patients. Seven tumors were from patients who showed intrinsic resistance to the EGFR-TKIs, gefitinib or erlotinib. Another seven tumors were from patients who showed acquired resistance to EGFR-TKIs (Figure 6a). Of 42 EGFR-TKI naive tumors, the presence of Aki1 protein was scored as 2+ in 31 tumors (74%), 1+ in 8 tumors (19%), and – in 3 tumors (7%). Aki1 protein was detected diffusely in all of seven tumors with intrinsic resistance: 2+ in 4 (57%), 1+ in 3 (43%). Aki1 protein was detected diffusely in all of seven tumors with acquired resistance: 2+ in 6 (86%), 1+ in 1 (14%) (Figure 6a). Aki1 was detected in all tumors with acquired resistance, including four tumors with *EGFR* T790M mutation (Supplementary Table S1). These findings suggest involvement of Aki1 in EGFR-mediating signaling in lung cancer with *EGFR* mutations, including T790M gatekeeper mutation.

DISCUSSION

The results of the present study indicated that Aki1 constitutively associates with mutant EGFR even in the presence of EGFR-TKI. Silencing of *Aki1* induces apoptosis of *EGFR* mutant lung cancer cells, indicating that Aki1 has crucial roles in survival signal transduction in lung cancer cells with *EGFR* mutations. In a xenograft model, silencing of *Aki1* markedly inhibited growth of lung cancer cells with *EGFR* T790M gatekeeper mutation. Furthermore, Aki1 was frequently expressed in tumor cells of *EGFR* mutant lung cancer patients. Notably, it was detected in all tumors with acquired resistance to gefitinib or erlotinib, suggesting that Aki1 is an ideal target for *EGFR* mutant lung cancer, especially in cases with acquired EGFR-TKI resistance due to *EGFR* T790M gatekeeper mutation.

Although Aki1 associates with wild-type EGFR when activated by EGF,[25] it binds constitutively with mutant EGFR (Figure 1b).

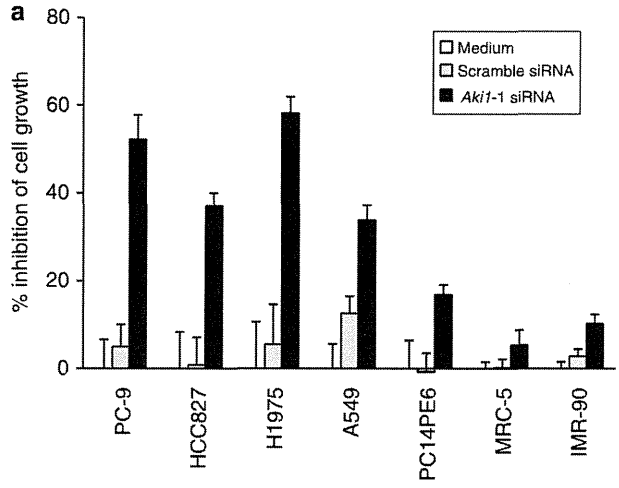

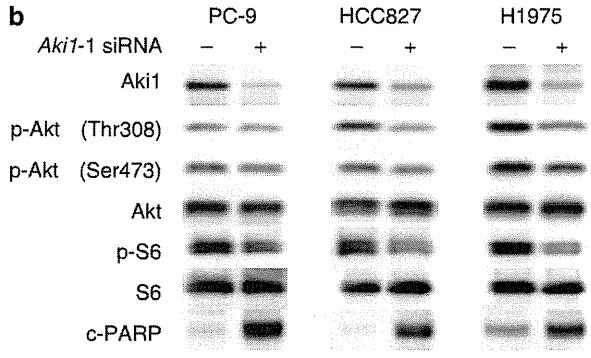

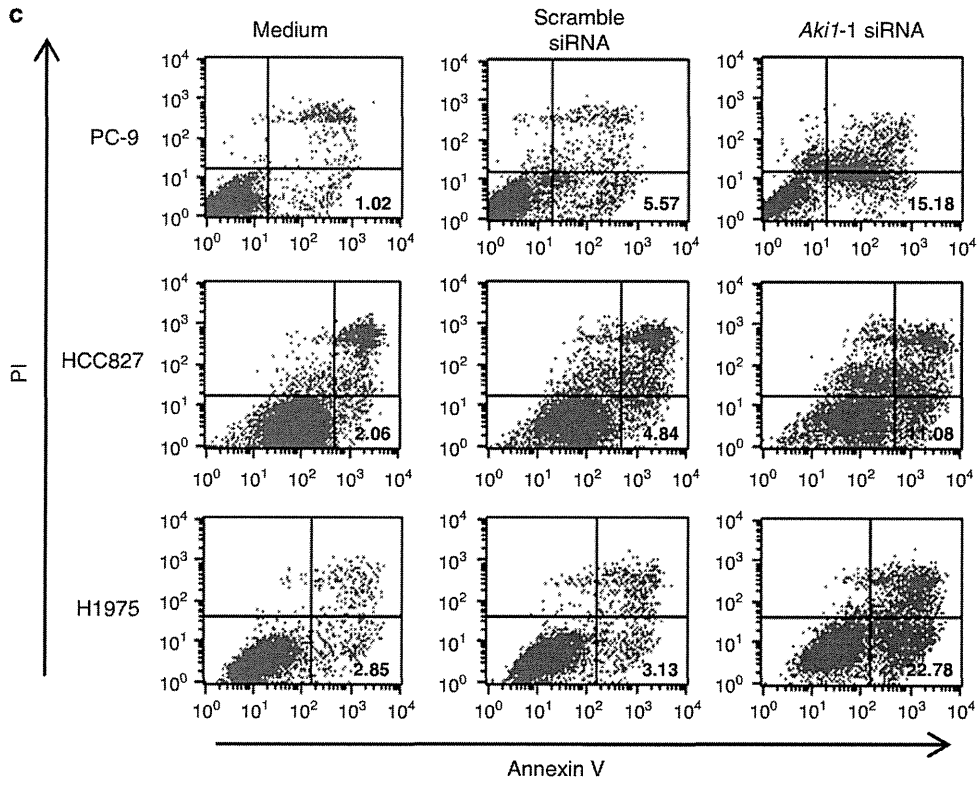

Previous studies indicated enhanced kinase activity and transformation capabilities of EGFR in the presence of L858R or exon 19 deletion mutation.[27,28] Crystal structure analysis of the L858R mutant EGFR showed that this substitution activates the kinase through disruption of autoinhibitory interactions, resulting in receptors with high kinase activity compared with wild-type EGFR.[10,29,30] Consistent with these observations, mutant EGFR was constitutively phosphorylated, while the levels were varied among cell lines used in the present study. Taken together, these results indicate that Aki1 binds constitutively with mutant EGFR because mutant EGFR is constitutively activated.

There is accumulating evidence that scaffold proteins maintain signaling specificity and facilitate the activation of pathway components.[24,31,32] We showed that Aki1 constitutively forms complexes with EGFR, PDK, and Akt in *EGFR* mutant lung cancer cells. As in EGFR non-mutated cancer cells,[25] Aki1 did not bind to IGF-1 R even after stimulation with IGF-1 in *EGFR* mutant cells, indicating that Aki1 is the determinant of receptor signaling selectivity for EGFR. In a phase II clinical trial, anti-IGF-1 R antibody improved the response rate of conventional chemotherapy in non-small-cell lung cancer.[33] However, the phase III trial was terminated because of a trend toward poorer overall survival in the group with anti-IGF-1 R antibody. A preliminary report of toxicity from a phase II trial with the anti-IGF-1 R antibody demonstrated severe adverse events, including hyperglycemia.[34]

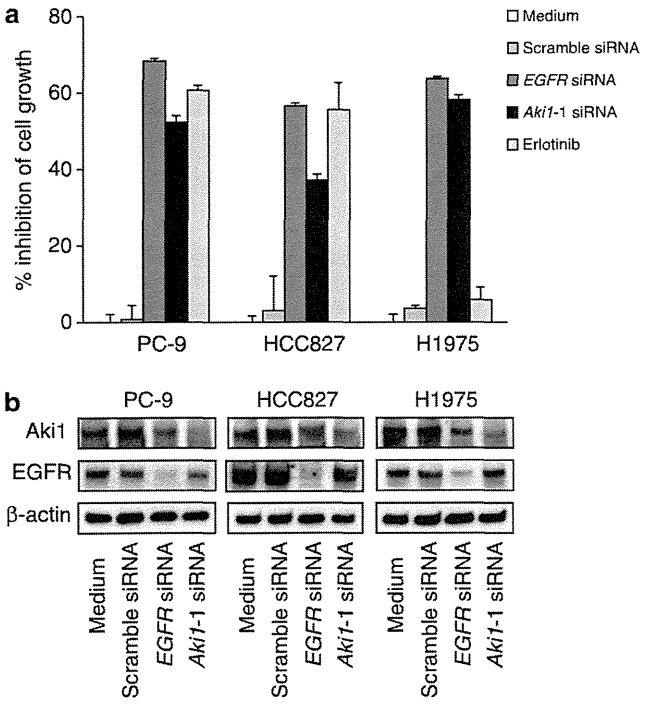

Figure 3. Comparison of efficacy between Aki1 knockdown and EGFR inhibition on cell viability. Cells were treated with *Aki1*-1 siRNA, *EGFR* siRNA, control scramble siRNA or erlotinib (1 μM). (**a**) After 72-h incubation, cell viability was determined by MTT assay. (**b**) After 24-h incubation, cells were lysed and the indicated proteins were detected by western blotting.

These findings indicated difficulty of targeting IGF-1 R in cancer. As Aki1 is an EGFR-selective scaffold protein, Aki1 inhibition may have advantage over non-selective inhibition of IGF-1 R or its downstream PI3K/Akt pathway in terms of safety.

EGFR-T790M gatekeeper mutation is associated with 50% of cases of acquired resistance to EGFR-TKIs in *EGFR* mutant lung cancer.[4,8,9] Recently, mutant-selective EGFR-TKIs were developed, which inhibit EGFR with not only activating mutations, such as exon 19 in-frame deletion and L858R point mutation, but also T790M resistant mutation.[35] As the inhibitors were reported to have less activity for non-mutated EGFR, they may overcome T790M-mediated resistance and reduce adverse events, including skin toxicity. We found not only that Aki1 inhibition further augmented the efficacy of mutant EGFR-selective TKI and irreversible EGFR-TKI, but also that Aki1 constitutively associated with EGFR regardless of treatment with EGFR-TKI. In addition, Aki1 was detected in all tumors with acquired resistance, including tumors with *EGFR* T790M mutation. Our findings indicated the necessity of development of efficient Aki1 inhibitors, and suggested that combined use of Aki1 inhibitors may increase the therapeutic effects and may reduce adverse events concerning EGFR blockade of new generation EGFR-TKIs in *EGFR* mutant lung cancer.

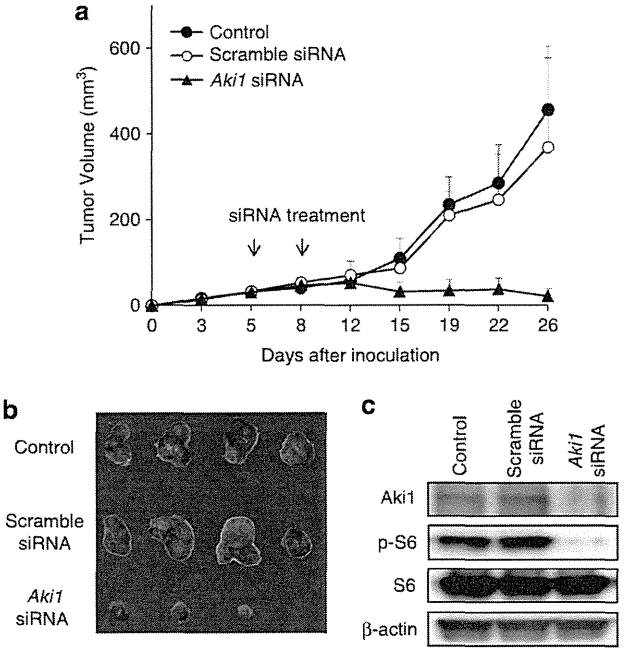

Figure 4. Therapeutic effects of *Aki1* knockdown against lung cancer cells with *EGFR* T790M secondary mutation *in vivo*. H1975 cells (5×10^6 cells per 100 μl of PBS) were injected subcutaneously into the flanks of 5-week-old male SCID mice. After cell inoculation, 50 μg of either scramble or *Aki1* siRNA complexed with invivofectamine was injected intratumorally on days 5 and 8. (**a**) Tumor size was measured twice a week and tumor volume was calculated as described in Materials and methods. (**b**) Macroscopic appearance of the tumors harvested on day 26. (**c**) The harvested tumors were examined for Aki1, and the inhibition of downstream signaling molecule, S6, in tumors by western blotting.

Figure 2. Effects of *Aki1* siRNA on cell viability and apoptosis in EGFR mutant human lung cancer cell lines. Cells were treated with *Aki1*-1 or control scramble siRNA. (**a**) After 72-h incubation, cell viability was determined by MTT assay. (**b**) After 24-h incubation with control scramble siRNA (lanes 1, 3 and 5) or *Aki1*-1 siRNA (lanes 2, 4 and 6), cells were lysed and the indicated proteins were detected by western blotting. (**c**) After 48-h incubation, cell apoptosis was determined with an Annexin V-FITC Apoptosis Detection Kit I. The numbers show percentages of early apoptotic cells.

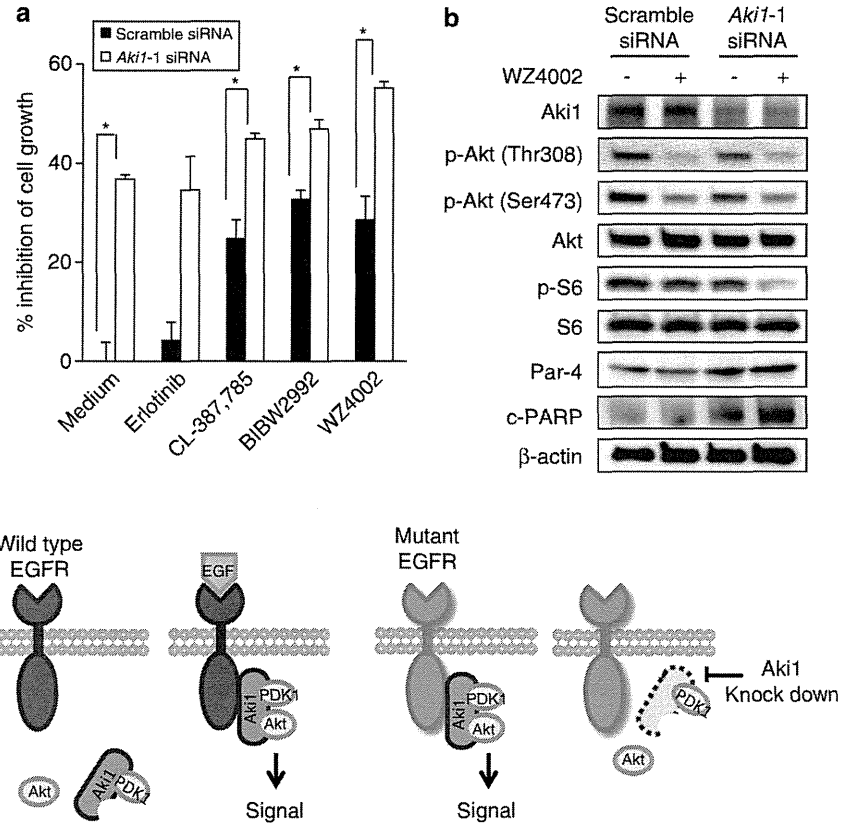

Figure 5. Effects of *Aki1* knockdown combined with new generation EGFR TKI in lung cancer with *EGFR* T790M secondary mutation. H1975 cells were treated with *Aki1*-1 or control scramble siRNA in the presence or absence of erlotinib (1 μM), CL-387, 785 (0.3 μM), BIBW2992 (0.1 μM) or WZ4002 (0.1 μM). (**a**) After 72-h incubation, cell viability was determined by MTT assay. $*P<0.01$, one-way ANOVA. (**b**) After 24-h incubation, cells were lysed and the indicated proteins were detected by western blotting. (**c**) Schema showing the role of Aki1 in cells with wild-type EGFR and mutant EGFR.

In conclusion, we demonstrated that Aki1 constitutively associates with EGFR activating mutation as well as T790M gatekeeper mutation has important roles as a determinant of receptor selective signaling for mutant EGFR, and mediates the survival signal to Akt. Our data provide a rationale for targeting Aki1 in *EGFR* mutant lung cancer patients, especially in cases with acquired resistance due to EGFR-T790M gatekeeper mutation. We are currently developing a drug delivery system for *Aki1* siRNA and small compounds with Aki1 inhibitory activity.

MATERIALS AND METHODS

Cell lines and reagents

The PC-9 and HCC827 human lung adenocarcinoma cell lines with EGFR-activating mutation (deletion in exon 19) were purchased from Immuno-Biological Laboratories (Gunma, Japan) and American Type Culture Collection (Manassas, VA, USA), respectively.[36] The H1975 human lung adenocarcinoma cell line with EGFR-L858R/T790M double mutation[10] was kindly provided by Dr John D Minna (University of Texas Southwestern Medical Center). The A549 human lung adenocarcinoma cell line, which expresses wild-type EGFR, was purchased from American Type Culture Collection. PC14PE6 human lung adenocarcinoma cell line, which expresses wild-type EGFR, was kindly provided by Dr Isaiah J Fidler (MD Anderson Cancer Center, Houston, TX, USA).[37] The human lung embryonic fibroblast MRC-5 (P30-35) and IMR-90 (P20-25) cell lines were obtained from RIKEN Cell Bank (Ibaraki, Japan). H1975, PC-9, HCC827, A549, and PC14PE6 cells were cultured in RPMI 1640, and MRC-5 and IMR-90 cells were cultured in Dulbecco's modified Eagle's medium supplemented with 10% fetal bovine serum (FBS), penicillin (100 units/ml) and streptomycin (50 μg/ml), in a humidified CO_2 incubator at 37 °C. All experiments were performed in medium supplemented with 10% FBS. Erlotinib hydrochloride was obtained from Roche Pharma AG (Basel, Switzerland). CL-387, 785 was purchased from Calbiochem (San Diego, CA, USA). BIBW2992 and WZ4002 were purchased from Seleck Chemicals (Houston, TX, USA). Human wild-type *Aki1* cDNA in the pFLAG-CMV-2 vector was generated previously.[25] RNAi-resistant *Aki1* cDNA in the pFLAG-CMV-2 vector was generated by mutating CAAACTC of Aki1 siRNA-targeting sequence to TAAGTTA without changing the amino acid sequence.

Immunoprecipitation and western blotting

Tumor cells were incubated in 10 ml of RPMI 1640 with 10% FBS for 1 h. The cells were then washed twice with phosphate-buffered saline (PBS), harvested in cell lysis buffer (20 mM Tris, pH 7.4, 150 mM NaCl, 1 mM EDTA, 1 mM EGTA, 1% Triton X-100, 2.5 mM sodium pyrophosphate, 1 mM β-glycerophosphate, 1 mM Na_3VO_4, 1 μg/ml leupeptin and 1 mM phenylmethylsulfonyl fluoride) and flash-frozen on dry ice. After allowing the cells to thaw, the cell lysates were collected with a rubber scraper, sonicated and centrifuged at 14 000 × *g* (4 °C for 20 min). The total protein concentration was measured using a Pierce BCA Protein Assay Kit (Pierce, Rockford, IL, USA). Aliquots of 400 μg of total proteins were immunoprecipitated with the appropriate antibodies. In some experiments, tumor cells were incubated in 10 ml of RPMI 1640 with 0.1% FBS in the presence or absence of erlotinib (0.3 μM), CL-387, 785 (0.3 μM) for 48 h. In other experiments, tumor cells were incubated in 10 ml of RPMI 1640 with 0.1% FBS in the presence or absence of EGF (50 ng/ml) or IGF-1 (50 ng/ml) for 10 min. In some experiments, tumor cells were transfected with RNAi for 24 h incubation and then incubated in 10 ml of RPMI 1640 with 10% FBS in the presence or absence of WZ4002 (0.1 μM) for 1 h. Immune complexes were recovered with Protein G-Sepharose beads (Zymed Laboratories, San Francisco, CA, USA). For western blotting assay, immunoprecipitates or cell lysates were subjected to SDS–PAGE (Bio-Rad, Hercules, CA, USA) and the proteins were then transferred onto polyvinylidene difluoride membranes (Bio-Rad). The membranes were blocked with Blocking One (Nacalai Tesque, Kyoto, Japan) for 1 h at room temperature, and the blots were then incubated at 4 °C overnight with anti-phospho-EGFR (Y1068), anti-Akt

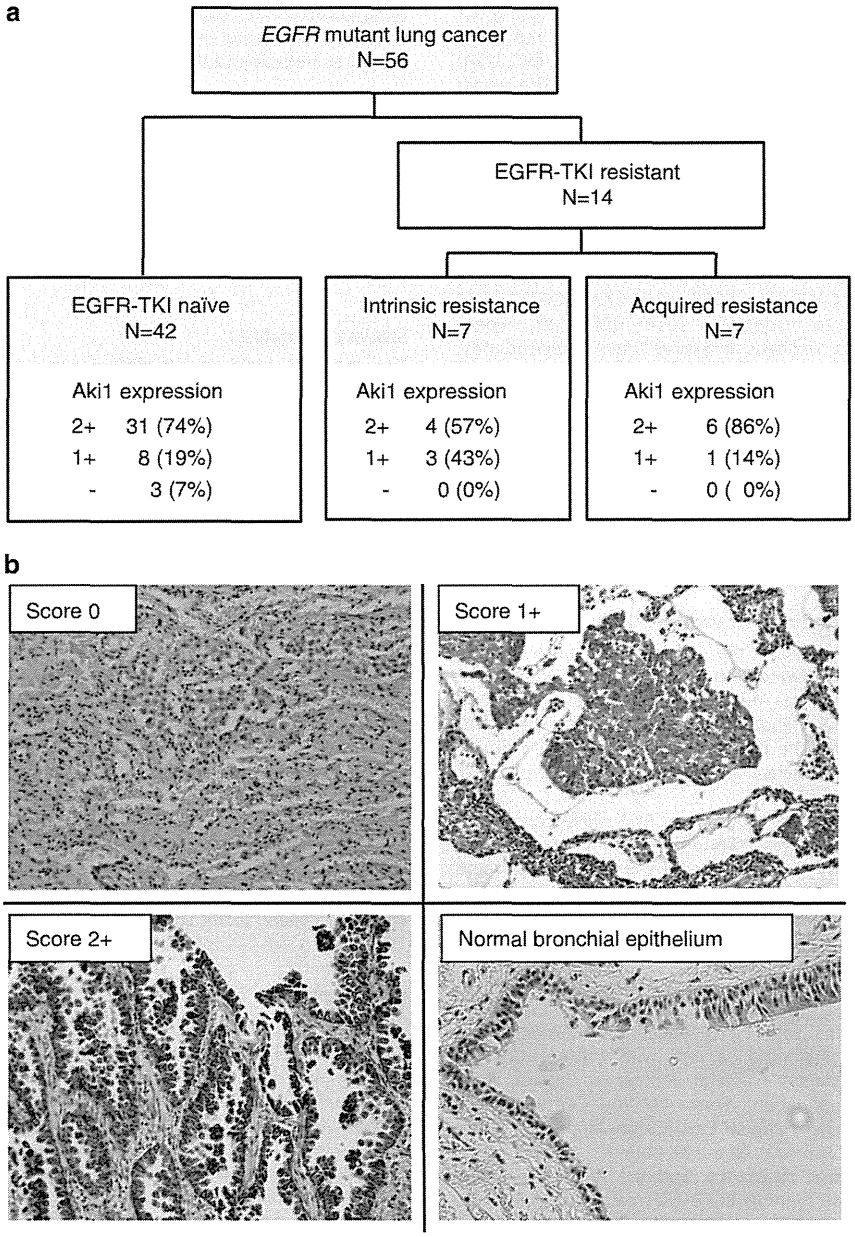

Figure 6. Aki1 is frequently expressed in *EGFR* mutant lung cancer. Clinical specimens from EGFR mutant lung cancer patients were stained for Aki1 by immunohistochemistry. (**a**) A total of 56 tumor specimens with EGFR-activating mutations were obtained from 56 lung adenocarcinoma patients. Of the 56 patients, 42 were EGFR-TKI naive, 7 tumors were from patients who showed intrinsic resistance to the EGFR-TKIs, gefitinib or erlotinib. Another seven tumors were from patients who showed acquired resistance to EGFR-TKIs. Of 42 EGFR-TKI naive tumors, the presence of Aki1 protein was scored as 2+ in 31 tumors (74%), 1+ in 8 tumors (19%) and – in 3 tumors (7%). Aki1 protein was detected diffusely in all of seven tumors with intrinsic resistance: 2+ in 4 (57%), 1+ in 3 (43%). Aki1 protein was detected diffusely in all of seven tumors with acquired resistance: 2+ in 6 (86%), 1+ in 1 (14%). (**b**) Representative staining results are shown.

(40D4), anti-phospho-Akt (Thr308), anti-phospho-Akt (Ser473), anti-Par-4, anti-cleaved PARP (Asp214), anti-phospho-S6 ribosomal protein (Ser235/236), anti-S6 ribosomal protein (5G10), anti-phospho-IGF-1 R (Tyr1131), DYKDDDDK (FLAG) tag antibody or anti-β-actin (13E5) antibodies (1:1000 dilution; Cell Signaling Technology, Danvers, MA, USA), anti-Aki1 (1:1000 dilution; Bethyl Laboratories, Montgomery, TX, USA), anti-PDK1 (1:1000 dilution; Santa Cruz Biotechnology, Santa Cruz, CA, USA), and anti-human EGFR (1 μg/ml) or anti-human IGF-1 R (0.1 μg/ml) antibody (R&D Systems, Minneapolis, MN, USA). After washing three times, the membranes were incubated for 1 h at room temperature with secondary Ab (horseradish peroxidase-conjugated species-specific Ab). Immunoreactive bands were visualized with SuperSignal West Dura Extended Duration Substrate Enhanced Chemiluminescent Substrate (Pierce). Each experiment was performed at least three times independently.

RNAi and proliferation assay *in vitro*

Duplexed Stealth RNAi (Invitrogen) against *Aki1*, *EGFR* and Stealth RNAi Negative Control Low GC Duplex no. 3 (Invitrogen, Carlsbad, CA, USA) were used for RNAi assay. Briefly, aliquots of 1×10^5 cells in 2 ml of antibiotic-free medium were plated on six-well plates and incubated at 37 °C for 24 h. The cells were then transfected with siRNA (250 pmol) or scramble RNA using Lipofectamine 2000 (5 μl) in accordance with the manufacturer's instructions (Invitrogen). After 24 h, the cells were washed twice with PBS. These partial cells were then used for western blotting and cell apoptosis assay. For proliferation assay, the cells were reseeded at 2×10^3 per well in 96-well plates, and incubated in antibiotic-containing RPMI 1640 with 10% FBS for 48 h. Otherwise, after 24 h of incubation, erlotinib (1 μM), CL-387, 785 (0.3 and 1 μM), BIBW2992 (0.1 and 0.3 μM) or WZ4002 (0.1, 0.3 μM) was added to each well, and incubation was continued for a further 48 h. These

cells were then used for proliferation assay, which was measured using the MTT (3-(4,5-dimethylthiazol-2-yl)-2,5-diphenyl tetrazolium) dye reduction method. An aliquot of MTT solution (2 mg/ml; Sigma, St Louis, MO, USA) was added to each well followed by incubation for 2 h at 37 °C. The media were removed and the dark blue crystals in each well were dissolved in 100 μl of dimethyl sulfoxide (DMSO). Absorbance was measured with an MTP-120 microplate reader (Corona Electric, Ibaraki, Japan) at test and reference wavelengths of 550 nm and 630 nm, respectively. The percentage of growth is shown relative to untreated controls.

Aki1 and *EGFR* knockdown were confirmed by western blotting analysis. The target sequences of siRNAs were as follows: *Aki1*-1, 5′-AGGAGCAGTT CAAACTCTGCATCAA-3′ (corresponding to nucleotides 2125–2168); *Aki1*-2, 5′-AACAAAGACAUCCAGAUCGCCAGGG-3′; *EGFR*, 5′-CGGAATAGGTATTGGT GAATTTAAA-3′ (corresponding to nucleotides 1014–1038). Each experiment was performed at least in triplicate, and three times independently.

Cell apoptosis assay

Cell apoptosis induced by *Aki1*-1 siRNA, *Aki1*-2 siRNA or Scramble siRNA was detected with an Annexin V-FITC Apoptosis Detection Kit I (BD Biosciences Pharmingen, Heidelberg, Germany) in accordance with the manufacturer's protocols as we described previously.[36] The analysis was performed on a FACSCalibur flow cytometer with Cell Quest software (Becton Dickinson, Franklin Lakes, NJ, USA).

Xenograft studies in SCID mice and *in vivo* RNAi

Suspensions of H1975 cells (5×10^6 cells per 100 μl of PBS) were injected subcutaneously into the flanks of 5-week-old male SCID mice (Nihon Clea Co., Ltd, Tokyo, Japan). Tumor size was measured using digital calipers and tumor volume was calculated as $0.5 \times \text{length} \times (\text{width})^2$. All animal experiments complied with the Guidelines for the Institute for Experimental Animals, Kanazawa University Advanced Science Research Center (approval no. AP-081088).

After cell inoculation, 50 μg of either scramble or Aki1 siRNA complexed with Invivofectamine (Invitrogen) was injected intratumorally on days 5 and 8. Tumors were harvested on day 26. siRNA and Invivofectamine complex was prepared in accordance with the manufacturer's instructions (Invitrogen). Aki1 knockdown in tumor tissue was confirmed by western blotting analysis.

Patients

A total of 56 tumor specimens with EGFR-activating mutations were obtained from 56 lung adenocarcinoma patients with written informed consent at the Kanazawa University Hospital (Kanazawa, Japan), Aichi Cancer Center Hospital (Nagoya, Japan), Osaka Medical Center (Osaka, Japan) and National Cancer Center Hospital East (Chiba, Japan) in studies with Institutional Review Board approval. Of the 56 patients, 42 were EGFR-TKI naive, seven showed intrinsic resistance, and the remaining seven patients showed partial response to initial EGFR-TKI treatment. As intrinsic resistance is not yet clearly defined, in the present study, we defined intrinsic resistant tumors as follows: response to treatment with an EGFR-TKI as defined by either documented stable disease or progressive disease (RECIST). Data for specimens from the seven patients who showed intrinsic resistance were obtained before EGFR-TKI treatment. For the seven patients who showed acquired resistance, tumor specimens were available after the development of acquired resistance to EGFR-TKI. Tumors with acquired resistance were defined as described previously.[38] Four of seven tumors from seven patients who showed acquired resistance had T790M secondary mutation.

Histology and immunohistochemistry

Immunohistochemical staining was carried out on formalin-fixed, paraffin-embedded tissue sections of lung adenocarcinoma specimens. Sections 4-μm thick were deparaffinized in xylene and rehydrated in decreasing concentrations of ethanol. After blocking the endogenous peroxidase activity with 3% aqueous H_2O_2 solution for 12 min, the sections were treated with 5% normal horse serum. The sections were then reacted with primary antibody (1:100 dilution, rabbit polyclonal anti-CC2D1A antibody; Sigma-Aldrich Corp., St Louis, MO, USA) at 4 °C overnight. After washing with PBS, the sections were treated with biotin-conjugated anti-rabbit IgG (1:200 dilution) for 30 min at room temperature and allowed to react for 30 min with avidin–biotin–peroxidase complex (ABC) using a Vectastain ABC kit (Vector Laboratories, Burlingame, CA, USA). The DAB (3,3′-diaminobenzidine tetrahydrochloride) Liquid System (DakoCytomation, Glostrup, Denmark) was used to detect immunostaining. Omission of primary antibodies served as negative control.

Evaluation of immunohistochemical results

Aki1 immunoreactivity was evaluated as the percentage of cancer cells with positive cytoplasmic staining (0, <5%; 1+, 5%–50%; 2+, >50%). Positive cells were defined as those with staining intensity that was the same or greater than that of normal bronchial epithelium (Figure 6b). Evaluation was performed independently by two investigators (TY, HU) who were blind to individual clinical information about specimens.

Statistical analysis

The statistical significance of differences was analyzed by one-way ANOVA performed with GraphPad Prism Ver. 4.01 (GraphPad Software, Inc., San Diego, CA, USA). In all analyses, $P<0.05$ was taken to indicate statistical significance.

CONFLICT OF INTEREST

Seiji Yano received honoraria from Chugai Pharmaceutical Co., Ltd. and AstraZeneca. Seiji Yano received research funding from Pharmaceutical Co., Ltd., Kyowa Hakko Kirin Co., Ltd. and Eisai Co., Ltd.

ACKNOWLEDGEMENTS

We thank Dr John D Minna (University of Texas Southwestern Medical Center) and Dr Isaiah J Fidler (MD Anderson Cancer Center, Houston, TX, USA) for kindly provided by H1975 and PC14PE6, respectively. We thank Mrs Takayuki Nakagawa and Kenji Kita (Cancer Research Institute, Kanazawa University) for technical assistance and fruitful discussion. This work was supported in part by the Grant-in-Aid for Cancer Research from the Ministry of Health, Labor and Welfare (M Noguchi, 16-1) and was supported by Grants-in-Aid for Cancer Research (T Yamada, 23790902 and S Yano, 21390256) and Scientific Research on Innovative Areas 'Integrative Research on Cancer Microenvironment Network' (S Yano, 22112010) from the Ministry of Education, Culture, Sports, Science, and Technology of Japan.

REFERENCES

1 Pao W, Chmielecki J. Rational, biologically based treatment of EGFR-mutant non-small-cell lung cancer. *Nat Rev Cancer* 2010; **10**: 760–774.
2 Maemondo M, Inoue A, Kobayashi K, Sugawara S, Oizumi S, Isobe H *et al.* Gefitinib or chemotherapy for non-small-cell lung cancer with mutated EGFR. *N Engl J Med* 2010; **362**: 2380–2388.
3 Mitsudomi T, Morita S, Yatabe Y, Negoro S, Okamoto I, Tsurutani J *et al.* Gefitinib versus cisplatin plus docetaxel in patients with non-small-cell lung cancer harbouring mutations of the epidermal growth factor receptor (WJTOG3405): an open label, randomised phase 3 trial. *Lancet Oncol* 2010; **11**: 121–128.
4 Mitsudomi T, Yatabe Y. Mutations of the epidermal growth factor receptor gene and related genes as determinants of epidermal growth factor receptor tyrosine kinase inhibitors sensitivity in lung cancer. *Cancer Sci* 2007; **98**: 1817–1824.
5 Gorre ME, Mohammed M, Ellwood K, Hsu N, Paquette R, Rao PN *et al.* Clinical resistance to STI-571 cancer therapy caused by BCR-ABL gene mutation or amplification. *Science* 2001; **293**: 876–880.
6 Yauch RL, Dijkgraaf GJ, Alicke B, Januario T, Ahn CP, Holcomb T *et al.* Smoothened mutation confers resistance to a Hedgehog pathway inhibitor in medulloblastoma. *Science* 2009; **326**: 572–574.
7 Choi YL, Soda M, Yamashita Y, Ueno T, Takashima J, Nakajima T *et al.* EML4-ALK mutations in lung cancer that confer resistance to ALK inhibitors. *N Engl J Med* 2010; **363**: 1734–1739.
8 Kobayashi S, Boggon TJ, Dayaram T, Jänne PA, Kocher O, Meyerson M *et al.* EGFR mutation and resistance of non-small-cell lung cancer to gefitinib. *N Engl J Med* 2005; **352**: 786–792.
9 Pao W, Miller VA, Politi KA, Riely GJ, Somwar R, Zakowski MF *et al.* Acquired resistance of lung adenocarcinomas to gefitinib or erlotinib is associated with a second mutation in the EGFR kinase domain. *PLoS Med* 2005; **2**: e73.
10 Yun CH, Mengwasser KE, Toms AV, Woo MS, Greulich H, Wong KK *et al.* The T790M mutation in EGFR kinase causes drug resistance by increasing the affinity for ATP. *Proc Natl Acad Sci USA* 2008; **105**: 2070–2075.
11 Kwak EL, Sordella R, Bell DW, Godin-Heymann N, Okimoto RA, Brannigan BW *et al.* Irreversible inhibitors of the EGF receptor may circumvent acquired resistance to gefitinib. *Proc Natl Acad Sci USA* 2005; **102**: 7665–7670.

12 Kobayashi S, Ji H, Yuza Y, Meyerson M, Wong KK, Tenen DG *et al.* An alternative inhibitor overcomes resistance caused by a mutation of the epidermal growth factor receptor. *Cancer Res* 2005; **65**: 7096–7101.
13 Yu Z, Boggon TJ, Kobayashi S, Jin C, Ma PC, Dowlati A *et al.* Resistance to an irreversible epidermal growth factor receptor (EGFR) inhibitor in EGFR-mutant lung cancer reveals novel treatment strategies. *Cancer Res* 2007; **67**: 10417–10427.
14 Engelman JA, Zejnullahu K, Gale CM, Lifshits E, Gonzales AJ, Shimamura T *et al.* PF00299804, an irreversible pan-ERBB inhibitor, is effective in lung cancer models with EGFR and ERBB2 mutations that are resistant to gefitinib. *Cancer Res* 2007; **67**: 11924–11932.
15 Li D, Ambrogio L, Shimamura T, Kubo S, Takahashi M, Chirieac LR *et al.* BIBW2992, an irreversible EGFR/HER2 inhibitor highly effective in preclinical lung cancer models. *Oncogene* 2008; **27**: 4702–4711.
16 Sequist LV, Besse B, Lynch TJ, Miller VA, Wong KK, Gitlitz B *et al.* Neratinib, an irreversible pan-ErbB receptor tyrosine kinase inhibitor: results of a phase II trial in patients with advanced non-small-cell lung cancer. *J Clin Oncol* 2010; **28**: 3076–3083.
17 Janjigian YY, Groen HJM, Horn L, Smit EF, Yali Fu FW, Shahidi M *et al.* Activity and tolerability of afatinib (BIBW 2992) and cetuximab in NSCLC patients with acquired resistance to erlotinib or gefitinib. *J Clin Oncol* 2011; **29**: 7525.
18 Sordella R, Bell DW, Haber DA, Settleman J. Gefitinib-sensitizing EGFR mutations in lung cancer activate anti-apoptotic pathways. *Science* 2004; **305**: 1163–1167.
19 Engelman JA, Jänne PA. Mechanisms of acquired resistance to epidermal growth factor receptor tyrosine kinase inhibitors in non-small cell lung cancer. *Clin Cancer Res* 2008; **14**: 2895–2899.
20 Morrison DK. KSR: a MAPK scaffold of the Ras pathway? *J Cell Sci* 2001; **114**: 1609–1612.
21 Ishibe S, Joly D, Zhu X, Cantley LG. Phosphorylation-dependent paxillin-ERK association mediates hepatocyte growth factor-stimulated epithelial morphogenesis. *Mol Cell* 2003; **12**: 1275–1285.
22 Yeung K, Seitz T, Li S, Janosch P, McFerran B, Kaiser C *et al.* Suppression of Raf-1 kinase activity and MAP kinase signalling by RKIP. *Nature* 1999; **401**: 173–177.
23 Whitmarsh AJ. The JIP family of MAPK scaffold proteins. *Biochem Soc Trans* 2006; **34**: 828–832.
24 Kolch W. Coordinating ERK/MAPK signalling through scaffolds and inhibitors. *Nat Rev Mol Cell Biol* 2005; **6**: 827–837.
25 Nakamura A, Naito M, Tsuruo T, Fujita N. Freud-1/Aki1, a novel PDK1-interacting protein, functions as a scaffold to activate the PDK1/Akt pathway in epidermal growth factor signaling. *Mol Cell Biol* 2008; **28**: 5996–6009.
26 Mouri A, Sasaki A, Watanabe K, Sogawa C, Kitayama S, Mamiya T *et al.* MAGE-D1 regulates expression of depression-like behavior through serotonin transporter ubiquitylation. *J Neurosci* 2012; **32**: 4562–4580.
27 Godin-Heymann N, Bryant I, Rivera MN, Ulkus L, Bell DW, Riese 2nd DJ *et al.* Oncogenic activity of epidermal growth factor receptor kinase mutant alleles is enhanced by the T790M drug resistance mutation. *Cancer Res* 2007; **67**: 7319–7326.
28 Mulloy R, Ferrand A, Kim Y, Sordella R, Bell DW, Haber DA *et al.* Epidermal growth factor receptor mutants from human lung cancers exhibit enhanced catalytic activity and increased sensitivity to gefitinib. *Cancer Res* 2007; **67**: 2325–2330.
29 Yun CH, Boggon TJ, Li Y, Woo MS, Greulich H, Meyerson M *et al.* Structures of lung cancer-derived EGFR mutants and inhibitor complexes: mechanism of activation and insights into differential inhibitor sensitivity. *Cancer Cell* 2007; **11**: 217–227.
30 Carey KD, Garton AJ, Romero MS, Kahler J, Thomson S, Ross S *et al.* Kinetic analysis of epidermal growth factor receptor somatic mutant proteins shows increased sensitivity to the epidermal growth factor receptor tyrosine kinase inhibitor, erlotinib. *Cancer Res* 2006; **66**: 8163–8171.
31 Clapéron A, Therrien M. KSR and CNK: two scaffolds regulating RAS-mediated RAF activation. *Oncogene* 2007; **26**: 3143–3158.
32 Dhanasekaran DN, Kashef K, Lee CM, Xu H, Reddy EP. Scaffold proteins of MAP-kinase modules. *Oncogene* 2007; **26**: 3185–3202.
33 Karp DD, Paz-Ares LG, Novello S, Haluska P, Garland L, Cardenal F *et al.* Phase II study of the anti-insulin-like growth factor type 1 receptor antibody CP-751,871 in combination with paclitaxel and carboplatin in previously untreated, locally advanced, or metastatic non-small-cell lung cancer. *J Clin Oncol* 2009; **27**: 2516–2522.
34 Neal JW, Sequist LV. Exciting new targets in lung cancer therapy: ALK, IGF-1 R, HDAC, and Hh. *Curr Treat Options Oncol* 2010; **11**: 36–44.
35 Zhou W, Ercan D, Chen L, Yun CH, Li D, Capelletti M *et al.* Novel mutant-selective EGFR kinase inhibitors against EGFR T790M. *Nature* 2009; **462**: 1070–1074.
36 Yano S, Wang W, Li Q, Matsumoto K, Sakurama H, Nakamura T *et al.* Hepatocyte growth factor induces gefitinib resistance of lung adenocarcinoma with epidermal growth factor receptor-activating mutations. *Cancer Res* 2008; **68**: 9479–9487.
37 Yano S, Shinohara H, Herbst RS, Kuniyasu H, Bucana CD, Ellis LM *et al.* Production of experimental malignant pleural effusions is dependent on invasion of the pleura and expression of vascular endothelial growth factor/vascular permeability factor by human lung cancer cells. *Am J Pathol* 2000; **157**: 1893–1903.
38 Jackman D, Pao W, Riely GJ, Engelman JA, Kris MG, Jänne PA *et al.* Clinical definition of acquired resistance to epidermal growth factor receptor tyrosine kinase inhibitors in non-small-cell lung cancer. *J Clin Oncol* 2010; **28**: 357–360.

Supplementary Information accompanies the paper on the Oncogene website (http://www.nature.com/onc)

Published OnlineFirst February 4, 2013; DOI: 10.1158/0008-5472.CAN-12-3479

Priority Report

Cancer Research

EGFR-TKI Resistance Due to *BIM* Polymorphism Can Be Circumvented in Combination with HDAC Inhibition

Takayuki Nakagawa[1,4], Shinji Takeuchi[1], Tadaaki Yamada[1], Hiromichi Ebi[1], Takako Sano[1], Shigeki Nanjo[1], Daisuke Ishikawa[1], Mitsuo Sato[2], Yoshinori Hasegawa[2], Yoshitaka Sekido[3], and Seiji Yano[1]

Abstract

BIM (BCL2L11) is a BH3-only proapoptotic member of the Bcl-2 protein family. BIM upregulation is required for apoptosis induction by EGF receptor (EGFR) tyrosine kinase inhibitors (EGFR-TKI) in *EGFR*-mutant forms of non–small cell lung cancer (NSCLC). Notably, a *BIM* deletion polymorphism occurs naturally in 12.9% of East Asian individuals, impairing the generation of the proapoptotic isoform required for the EGFR-TKIs gefitinib and erlotinib and therefore conferring an inherent drug-resistant phenotype. Indeed, patients with NSCLC, who harbored this host *BIM* polymorphism, exhibited significantly inferior responses to EGFR-TKI treatment than individuals lacking this polymorphism. In an attempt to correct this response defect in the resistant group, we investigated whether the histone deacetylase (HDAC) inhibitor vorinostat could circumvent EGFR-TKI resistance in *EGFR*-mutant NSCLC cell lines that also harbored the *BIM* polymorphism. Consistent with our clinical observations, we found that such cells were much less sensitive to gefitinib-induced apoptosis than *EGFR*-mutant cells, which did not harbor the polymorphism. Notably, vorinostat increased expression in a dose-dependent manner of the proapoptotic BH3 domain-containing isoform of BIM, which was sufficient to restore gefitinib death sensitivity in the *EGFR* mutant, EGFR-TKI–resistant cells. In xenograft models, while gefitinib induced marked regression via apoptosis of tumors without the *BIM* polymorphism, its combination with vorinostat was needed to induce marked regression of tumors with the *BIM* polymorphism in the same manner. Together, our results show how HDAC inhibition can epigenetically restore BIM function and death sensitivity of EGFR-TKI in cases of *EGFR*-mutant NSCLC where resistance to EGFR-TKI is associated with a common *BIM* polymorphism. *Cancer Res; 73(8); 2428–34.* ©*2013 AACR.*

Introduction

The EGF receptor (EGFR) tyrosine kinase inhibitors (TKI), gefitinib and erlotinib, have shown marked therapeutic effects against non–small cell lung cancer (NSCLC) with *EGFR*-activating mutations, such as exon 19 deletions and L858R point mutations (1). About 20% to 30% of patients, however, show intrinsic resistance to EGFR-TKIs despite having tumors harboring these *EGFR* mutations. In addition, patients who respond initially later develop acquired resistance to EGFR-TKIs after varying periods of time (2). Among the molecular mechanisms associated with acquired resistance to EGFR-TKIs are (i) gatekeeper mutations in *EGFR* (i.e., a T790M second mutation), (ii) activation of bypass signaling caused by *Met* amplification or hepatocyte growth factor overexpression, (iii) transformation to small-cell lung cancer, and (iv) epithelial-to-mesenchymal transition (3, 4). Several therapeutic strategies, including new generation EGFR-TKIs and the combination of an EGFR-TKI and a Met-TKI, have been evaluated clinically in patients with *EGFR*-mutant NSCLC who acquired resistance to EGFR-TKIs (2). The mechanisms of intrinsic resistance, however, remain poorly understood.

Recently, a *BIM* deletion polymorphism was reported to be a novel mechanism of intrinsic resistance to EGFR-TKIs (5). BIM, also called BCL2L11, is a proapoptotic protein and a member of the Bcl-2 family. Gene products (such as BIM_{EL}, BIM_L, and BIM_S) with a BH3 domain, which is essential for apoptosis induction, antagonize antiapoptotic proteins (such as Bcl-2, Bcl-X_L, and Mcl-1) and activate proapoptotic proteins (such as BAX and BAK), thereby inducing apoptosis (6, 7). Activation of BAX and BAK induce cytochrome *c* release into the cytoplasm and result in activation of the caspase cascade (8). BIM is pivotal in apoptosis induced by EGFR-TKIs in *EGFR*-mutant NSCLC cells (9). The expression and degradation of BIM is regulated mainly by the MEK-ERK pathway (10). The *BIM* deletion polymorphism is relatively common in East Asian populations (12.9%), with 0.5% of individuals being

Authors' Affiliations: [1]Division of Medical Oncology, Cancer Research Institute, Kanazawa University, Kanazawa, Ishikawa; [2]Department of Respiratory Medicine, Nagoya University; [3]Division of Molecular Oncology, Aichi Cancer Center Research Institute, Nagoya, Aichi; and [4]Tsukuba Research Laboratories, Eisai Co., ltd., Ibaraki, Japan

Note: Supplementary data for this article are available at Cancer Research Online (http://cancerres.aacrjournals.org/).

Corresponding Author: Seiji Yano, Division of Medical Oncology, Cancer Research Institute, Kanazawa University, 13-1 Takara-machi, Kanazawa, Ishikawa 9200934, Japan. Phone: 81-76-265-2780; Fax: 81-76-234-4524; E-mail: syano@staff.kanazawa-u.ac.jp

doi: 10.1158/0008-5472.CAN-12-3479

Published OnlineFirst February 4, 2013; DOI: 10.1158/0008-5472.CAN-12-3479

homozygous for this deletion. During the transcription of *BIM*, either exon 3 or exon 4, the latter of which encodes the BH3 domain, is spliced out due to the presence of a stop codon and a polyadenylation signal within exon 3 (11). The *BIM* deletion polymorphism involves the deletion of a 2903 bp fragment in intron 2 and results in the preferential splicing of exon 3 over exon 4, generating a *BIM* isoform that lacks the BH3 domain (5). A retrospective analysis in patients with *EGFR*-mutant NSCLC showed that progression-free survival (PFS) following EGFR-TKI treatment was significantly shorter in patients with the *BIM* polymorphism (6.6 months) than with wild-type *BIM* (11.9 months; ref.5). Another study in patients with *EGFR*-mutant NSCLC treated with EGFR-TKIs also reported that PFS was significantly shorter in patients with BIM-low (4.3 months) than BIM-high (11.3 months) expressing tumors (12), suggesting that reduced expression of BIM with a BH3 domain is associated with an unfavorable response to EGFR-TKIs. To date, however, no therapeutic strategy has yet been developed for patients with *EGFR*-mutant NSCLC with low BIM expression.

Histone deacetylase (HDAC) is an enzyme that regulates chromatin remodeling and is crucial in the epigenetic regulation of various genes (13). Many compounds targeting HDAC have been developed, including vorinostat, an HDAC inhibitor approved by the United States Food and Drug Administration (FDA) for the treatment of patients with cutaneous T-cell lymphoma (14). In mantle cell lymphoma (MCL) cell lines and in cells from patients with MCL, vorinostat induced histone hyperacetylation on promoter regions and consequent transcriptional activation of proapoptotic *BH3*-only genes, including BIM (15). Using *in vitro* and *in vivo* models, we assessed whether the combination of vorinostat and gefitinib restored the expression of BIM protein with a BH3 domain in *EGFR*-mutant NSCLC cells with the *BIM* polymorphism and overcame EGFR-TKI resistance associated with this polymorphism.

Materials and Methods

Cell lines and reagents

The NSCLC cell lines, PC-9, HCC827, and HCC2279, all of which have *EGFR* mutations, were obtained from Immuno-Biological Laboratories Co., ltd., the American Type Culture Collection (ATCC), and Dr. John Minna (University of Texas Southwestern Medical Center, Dallas, TX), respectively. PC-3 cells, established from a Japanese female patient with NSCLC and with an exon 19 deletion in *EGFR*, and differing from the prostate cancer cell line PC-3 (ATCC CRL1435), were purchased from Human Science Research Resource Bank (JCRB0077: http://cellbank.nibio.go.jp/~cellbank/cgi-bin/search_res_det.cgi?DB_NUM=1&ID=252 = 1&ID = 252). PC-3 and the other 3 cell lines were maintained in Dulbecco's Modified Eagle's Medium (DMEM) and RPMI-1640 medium, respectively, each supplemented with 10% FBS and antibiotics. All cells were passaged for less than 3 months before renewal from frozen, early-passage stocks. Cells were regularly screened for mycoplasma using a MycoAlert Mycoplasma Detection Kit (Lonza). The cell lines were authenticated at the laboratory of the National Institute of Biomedical Innovation (Osaka, Japan) by short tandem repeat analysis. Vorinostat and gefitinib were obtained from Selleck Chemicals and AstraZeneca, respectively.

Genotype and expression analysis of *BIM*

Genomic DNA was extracted from cells using DNeasy Blood and Tissue Kits (Qiagen), according to the manufacturer's protocol. Total RNA was extracted from cells using RNeasy PLUS Mini kits (Qiagen). PCR methods were used to detect the *BIM* deletion polymorphism in the samples and the level of expression of *BIM* isoforms (5).

Cell apoptosis

Cells (3×10^3) were seeded into each well of 96-well, white-walled plates, incubated overnight, and treated with the indicated compounds or vehicle [dimethyl sulfoxide (DMSO)] for 48 hours. Cellular apoptosis was analyzed with Caspase-Glo 3/7 assay kits (Promega), which measure caspase-3/7 activity, and PE-Annexin V Apoptosis Detection Kits (BD Biosciences, in accordance with the manufacturers' directions.

Apoptotic cells in tumor xenografts were detected by terminal deoxynucleotidyl transferase–mediated nick end labeling (TUNEL) staining, using the DeadEnd Fluorometric TUNEL system (Promega), according to the manufacturer's protocol.

RNA interference

Duplexed Stealth RNAi (Invitrogen) against *BIM* and Stealth RNAi-negative control low GC Duplex #3 (Invitrogen) were used for RNA interference (RNAi) assays as described (4). The siRNA target sequences were 5′-CAUGAGUUGUGACAAAUC-AACACAA-3′ and 5′-UUGUGUUGAUUUGUCACAACUCAUG-3′ for BIM #1, and 5′-UGAGUGUGACCGAGAAGGUAGACAA-3′ and 5′-UUGUCUACCUUCUCGGUCACACUCA-3′ for BIM #2.

Western blot analysis

Western blotting was conducted with antibodies against phospho-EGFR (Tyr1068), Akt, phospho-Akt (Ser473), cleaved PARP, cleaved caspase-3, histone H3, acetylated histone H3 (Lys27), BIM, and β-actin (Cell Signaling Technology); and against phospho-Erk1/2 (Thr202/Tyr204), Erk1/2, and EGFR (R&D Systems). Blots were subsequently incubated with horseradish peroxidase-conjugated secondary antibodies specific to mouse or rabbit immunoglobulin G, with signals detected by enhanced chemiluminescence (Pierce Biotechnology).

Subcutaneous xenograft models

Male BALB/cAJcl-nu/nu mice, ages 5 to 6 weeks, were obtained from CLEA Japan Inc and injected subcutaneously into their flanks with cultured tumor cells (5×10^6 cells/0.1 mL/mouse). When tumor volumes reached 100 to 200 mm^3, the mice were randomized and treated once daily with gefitinib and/or vorinostat. Each tumor was measured in 2 dimensions, and the volume was calculated using the formula: tumor volume (mm^3) = 1/2 × length (mm) × width $(mm)^2$. All animal experiments complied with the Guidelines for the Institute for Experimental Animals, Kanazawa University Advanced Science Research Center (approval No. AP-081088).

Published OnlineFirst February 4, 2013; DOI: 10.1158/0008-5472.CAN-12-3479

Statistical analysis

Between group differences were analyzed by one-way ANOVA. All statistical analyses were conducted using GraphPad Prism Ver. 4.01 (GraphPad Software, Inc.), with $P < 0.05$ considered statistically significant.

Results

EGFR-mutant NSCLC cell lines harboring the *BIM* deletion polymorphism have low susceptibility to gefitinib-induced apoptosis

We first examined the *BIM* deletion polymorphism in *EGFR*-mutant NSCLC cell lines by PCR. PC-9 and HCC827 had wild-type alleles, with a PCR product 4.2 kb in size. Consistent with a previous report (5), HCC2279 cells were heterozygous for the *BIM* deletion polymorphism, with PCR products 4.2 kb (wild-type) and 1.3 kb (2.9 kb deletion polymorphism) in size. Among the 7 additional cell lines with *EGFR* mutations (Supplementary Table S1), PC-3 was heterozygous for the *BIM* deletion polymorphism (Fig. 1A). Western blot analyses reveal that the expression of the proapoptotic BIM protein was markedly lower in PC-3 and HCC2279 than in PC-9 and HCC827 cells. Analysis of *BIM* isoform transcripts showed that cells with the *BIM* polymorphism expressed more exon 3- than exon 4-containing transcripts (Supplementary Fig. S1A and S1B). Treatment with gefitinib enhanced BIM expression, caspase-3/7 activities, and apoptosis in PC-9 and HCC827 cells much more than in PC-3 and HCC2279 cells (Fig. 1B; Supplementary Fig. S1C, S1D, and S2). Moreover, gefitinib did not increase caspase-3/7 activity in PC-9 and HCC827 cells treated with *BIM* siRNA (Fig. 1C), indicating the crucial role of BIM in apoptosis induction in *EGFR*-mutant NSCLC cells treated with EGFR-TKI. These observations clearly showed that *EGFR*-mutant NSCLC cells with the *BIM* deletion polymorphism are much less sensitive to gefitinib, as shown by induction of apoptosis, than cells with wild-type *BIM*.

Vorinostat upregulates BIM and efficiently induces apoptosis when combined with gefitinib

Because HDAC inhibition modulates the expression of various genes, including proapoptotic molecules (13), we hypothesized that the HDAC inhibitor, vorinostat, may sensitize *EGFR*-mutant NSCLC cells with the *BIM* polymorphism to gefitinib. In *EGFR*-mutated NSCLC cell lines, including PC-3 and HCC2279 cells, vorinostat dose dependently increased the expression of acetylated histone H3 and BIM with the BH3 domain (Fig. 2A, Supplementary Fig. S3A). We further explored whether the addition of vorinostat to gefitinib induced apoptosis in *EGFR*-mutant NSCLC cells with the *BIM* polymorphism (Fig. 2B and D). In HCC827 and PC-9 cells, which contain only wild-type *BIM*, gefitinib inhibited downstream signaling,

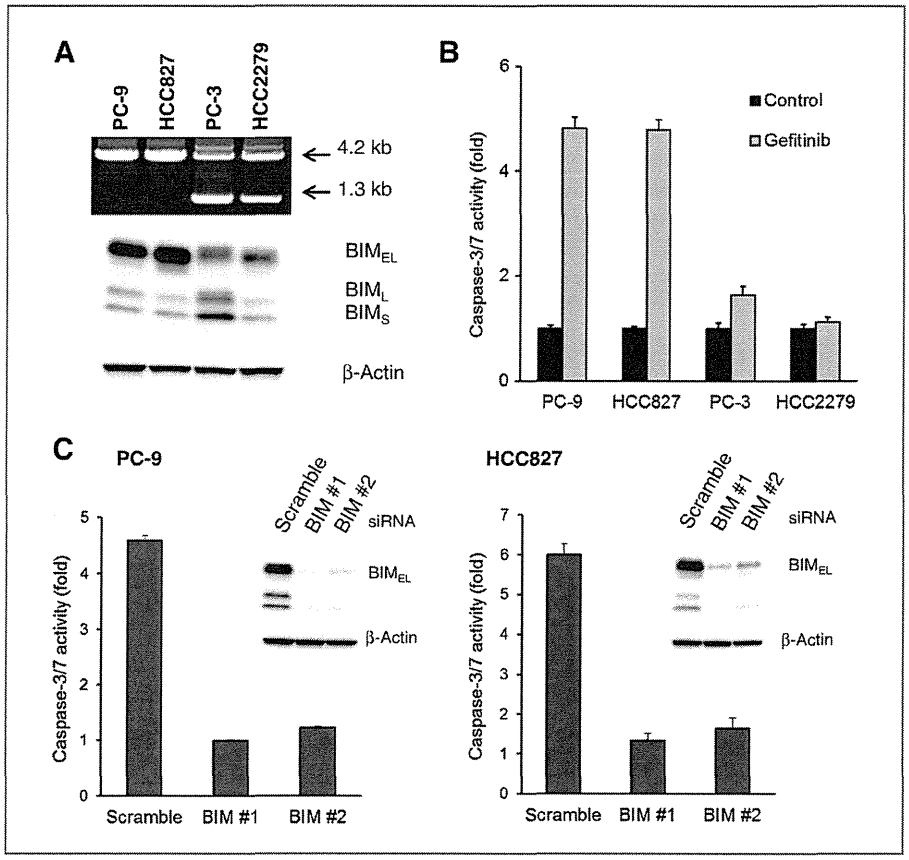

Figure 1. *EGFR*-mutated NSCLC cell lines harboring the *BIM* deletion polymorphism show low susceptibility to gefitinib-induced apoptosis. A, top, PCR products from the 4 *EGFR*-mutated NSCLC cell lines generated by primers flanking the deletion. PCR products 4.2 kb and 1.3 kb in size correspond to the alleles without and with the deletion, respectively, with the presence of both products indicating heterozygosity for the deletion polymorphism. Bottom, the levels of expression of the proteins BIM$_{EL}$, BIM$_L$, and BIM$_S$ in each cell line. B, cell lines were treated with gefitinib (1 μmol/L) or DMSO control for 48 hours, and the activity of caspase-3/7 was measured using Caspase-Glo3/7 assay kits. Each bar represents the mean ± SD. C, PC-9 (left) and HCC827 (right) cells were transfected with *BIM* or control siRNA for 24 hours before gefitinib (1 μmol/L) treatment for 48 hours, and the activity of caspase-3/7 was measured as in B. Each bar indicates the mean ± SD. Lysates were collected and proteins were analyzed by Western blotting.

Published OnlineFirst February 4, 2013; DOI: 10.1158/0008-5472.CAN-12-3479

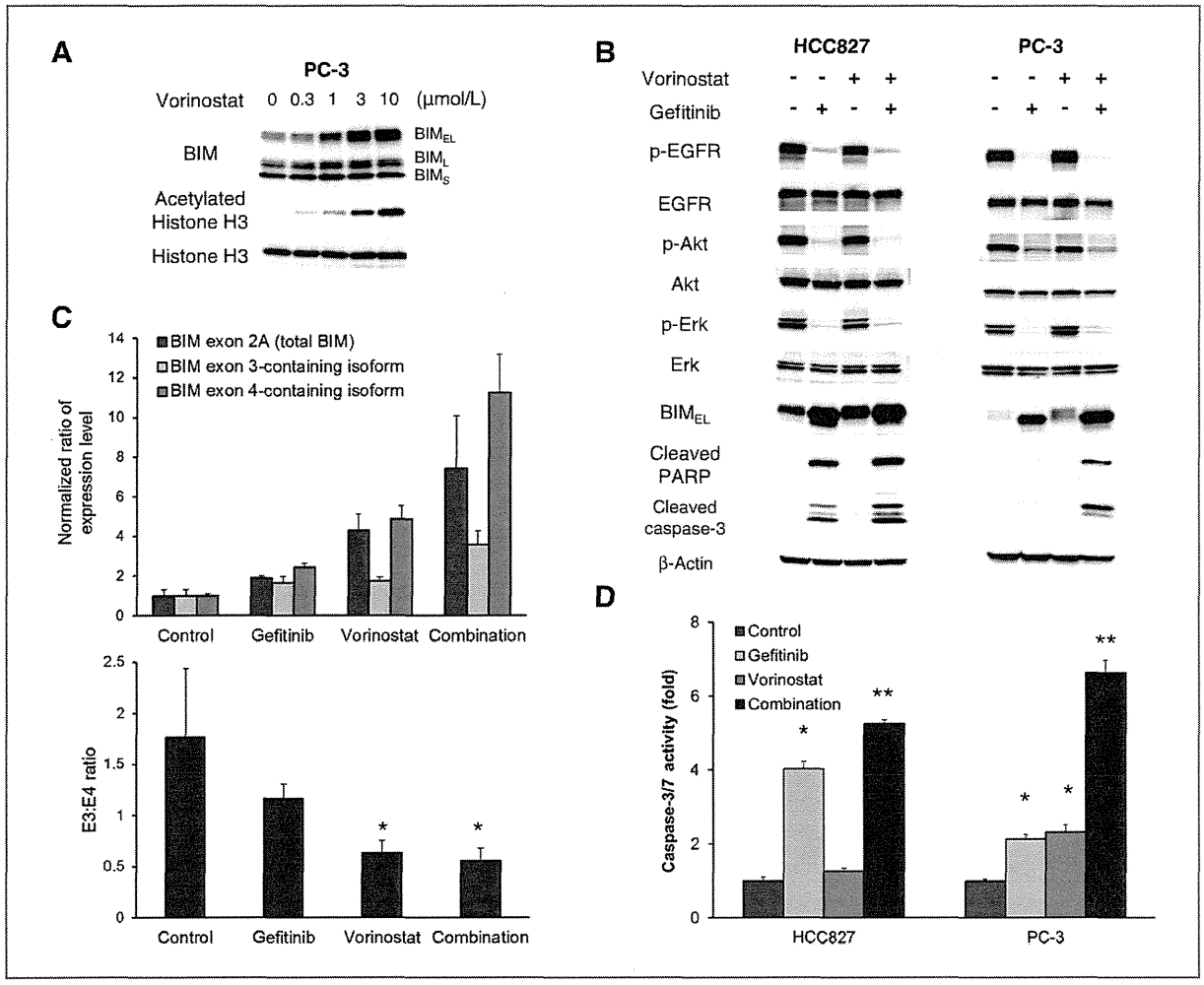

Figure 2. Upregulation of BIM by vorinostat enhances induction of apoptosis in *EGFR*-mutated NSCLC cell line with the *BIM* polymorphism. A, PC-3 cells were incubated with serial dilutions of vorinostat for 24 hours. The cell lysates were harvested and the indicated proteins were analyzed by Western blotting. B, HCC827 cells (left) and PC-3 cells (right) were incubated with gefitinib (1 μmol/L) and/or vorinostat (3 μmol/L) for 48 hours. The cell lysates were harvested and the indicated proteins were determined by Western blotting. C, PC-3 cells were treated with gefitinib (1 μmol/L) and/or vorinostat (3 μmol/L) for 12 hours. The amounts of the various transcripts containing exon 2A, 3, or 4 are expressed as normalized ratios relative to actin (top). Ratio of exon 3-containing transcripts to exon 4-containing transcripts in PC-3 cells after treatment with each compound. *, $P < 0.05$ versus control. Bar indicates the mean ± SD. D, apoptosis was analyzed by measurement of caspase-3/7 activity. *, $P < 0.05$ gefitinib or vorinostat versus control; **, $P < 0.05$ combination versus control and single agents. Bars represent the mean ± SD.

including the phosphorylation of EGFR, Erk, and Akt, resulting in apoptosis, as shown by the expression of cleaved PARP and cleaved caspase-3. The further addition of vorinostat augmented BIM expression and caspase-3/7 activity. In PC-3 and HCC2279 cells, which contain the *BIM* polymorphism, however, treatment with gefitinib alone induced minimal apoptosis, although the phosphorylation of EGFR, Erk, and Akt was inhibited, whereas the combination of vorinostat and gefitinib markedly increased the expression of BIM, as well as of cleaved PARP and cleaved caspase-3 (Fig. 2B and Supplementary Fig. S3B). This combination also augmented caspase-3/7 activity compared with that of gefitinib or vorinostat alone (Fig. 2D and Supplementary Fig. S3C), but this activation of caspase-3/7 was inhibited by knockdown of *BIM* (Supplementary Fig. S4A and S4B). Conversely, overexpression of BIM$_{EL}$ itself stimulated caspase-3/7 activities in cells with the *BIM* polymorphism, with these activities further enhanced by gefitinib treatment (Supplementary Fig. S4C and S4D). These results indicate that BIM mediates the activation of caspase-3/7 induced by gefitinib and vorinostat. Analysis of *BIM* transcripts revealed that vorinostat alone induced *BIM* mRNA, which was enhanced by the inclusion of gefitinib. Moreover, vorinostat treatment preferentially induced transcripts containing exon 4 over those containing exon 3 (Fig. 2C). These results indicate that the combination of vorinostat and gefitinib inhibits HDAC and increases the expression of BIM protein with the BH3 domain, thereby sensitizing *EGFR*-mutant NSCLC cells with the *BIM* polymorphism to apoptosis *in vitro*.

Published OnlineFirst February 4, 2013; DOI: 10.1158/0008-5472.CAN-12-3479

Combined treatment with vorinostat with gefitinib shrinks tumors produced by *EGFR*-mutant NSCLC cells with the *BIM* polymorphism

We next determined the *in vivo* efficacy of vorinostat and gefitinib. Gefitinib alone almost completely shrunk xenograft tumors induced by HCC827 cells (Fig. 3A). Although gefitinib monotherapy prevented the enlargement of tumors produced by PC-3 cells, which harbor the *BIM* polymorphism, it did not induce their complete regression, indicating that PC-3 cells remained less susceptible to gefitinib *in vivo*. Under these experimental conditions, vorinostat monotherapy inhibited tumor growth slightly, whereas the combination of vorinostat with gefitinib resulted in marked tumor shrinkage (Fig. 3B). None of the mice treated with these agents showed any macroscopic adverse effects, including loss of body weight (data not shown).

To clarify the mechanisms by which vorinostat and gefitinib act *in vivo*, we assessed tumor-cell apoptosis by TUNEL staining. Gefitinib treatment increased the number of apoptotic cells in HCC827 tumors but had little effect on PC-3 tumors (Fig. 4A and B), indicating that *EGFR*-mutant NSCLC cells with the *BIM* polymorphism are refractory to gefitinib-induced apoptosis *in vivo* as well as *in vitro*. Importantly, although vorinostat alone had little effect on apoptosis, the combination of vorinostat and gefitinib induced marked apoptosis in PC-3 tumors (Fig. 4A and B). Western blot analyses showed that gefitinib induced cleavage of caspase-3 in HCC827, but not in PC-3, tumors. In PC-3 tumors, treatment with gefitinib or vorinostat had little effect on caspase-3 cleavage, whereas their combination increased BIM expression and the cleavage of caspase-3 (Fig. 4C and D). These findings indicate that the combination of vorinostat and gefitinib increases BIM protein expression and induces tumor-cell apoptosis, thereby shrinking tumors produced by *EGFR*-mutant NSCLC cells with the *BIM* polymorphism.

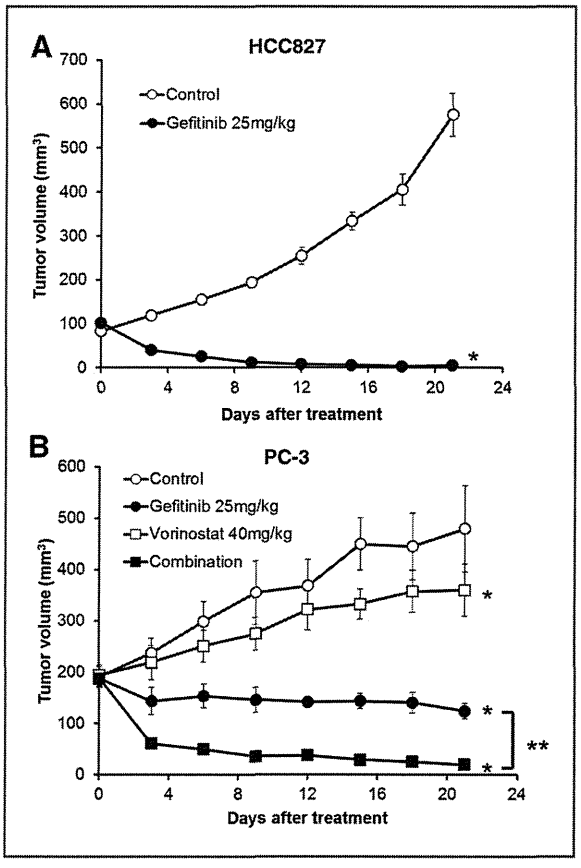

Figure 3. Antitumor activity of gefitinib and/or vorinostat in mouse xenograft models of HCC827 and PC-3 tumors. Nude mice bearing established tumors with HCC827 (A) or PC-3 (B) cells were treated with 25 mg/kg gefitinib and/or 40mg/kg vorinostat once daily for 21 days. Tumor volume was measured using calipers on the indicated days. Mean ± SE tumor volumes are shown for groups of 4 to 5 mice. *, $P < 0.05$ versus control, **, $P < 0.05$ versus gefitinib by one-way ANOVA.

Discussion

EGFR-mutant NSCLC cells with the *BIM* deletion polymorphism show impaired generation of BIM with the proapoptotic BH3 domain, as well as resistance to EGFR-TKI–induced apoptosis (5). We have shown here that treatment of cells with the combination of vorinostat, a HDAC inhibitor, and gefitinib, an EGFR-TKI, restored the expression of BIM protein with a BH3 domain (predominantly BIM_{EL}), induced apoptosis, and overcame gefitinib resistance *in vitro* and *in vivo*.

Although vorinostat preferentially induced expression of BIM containing the BH3 domain, its exact mechanisms of action remain unclear. The wild-type allele may be more susceptible to the effects of HDAC inhibition than the deletion allele due to differences in the acetylation status of these alleles. Alternatively, vorinostat may affect the splicing process, resulting in the production of exon 4- rather than exon 3-containing transcripts from the deletion polymorphism allele as HDAC has been found to affect the splicing of RNA (16).

Vorinostat has been shown to induce the expression of several genes other than *BIM* (13). However, we found that BIM was pivotal not only for gefitinib-induced apoptosis but also when combined with vorinostat. Moreover, the combination of vorinostat and gefitinib increased BIM expression and markedly induced apoptosis in PC-3 and HCC2279 cells. Collectively, these findings strongly suggest that vorinostat promotes gefitinib-induced apoptosis in *EGFR*-mutant NSCLC cells with the *BIM* polymorphism, primarily by increasing BIM expression. Several other mechanisms, including inhibition of epigenetic modifications leading to a drug-tolerant state (17) and transition of cancer cells from a resistant mesenchymal state to an E-cadherin–expressing epithelial state (18) may be also involved.

Both the *BIM* polymorphism and *EGFR* mutations are more prevalent in East Asian than in Caucasian populations. Few East Asian patients with *EGFR*-mutant NSCLC show a complete response to EGFR-TKIs (1). This incomplete response, including intrinsic resistance, may be due, in part, to low BIM expression associated with the *BIM* polymorphism (6). Our preclinical data indicate that vorinostat increases BIM even in *BIM*-wild type *EGFR*--mutant NSCLC cells. However, a clinical trial with erlotinib and entinostat, an HDAC inhibitor, in

Published OnlineFirst February 4, 2013; DOI: 10.1158/0008-5472.CAN-12-3479

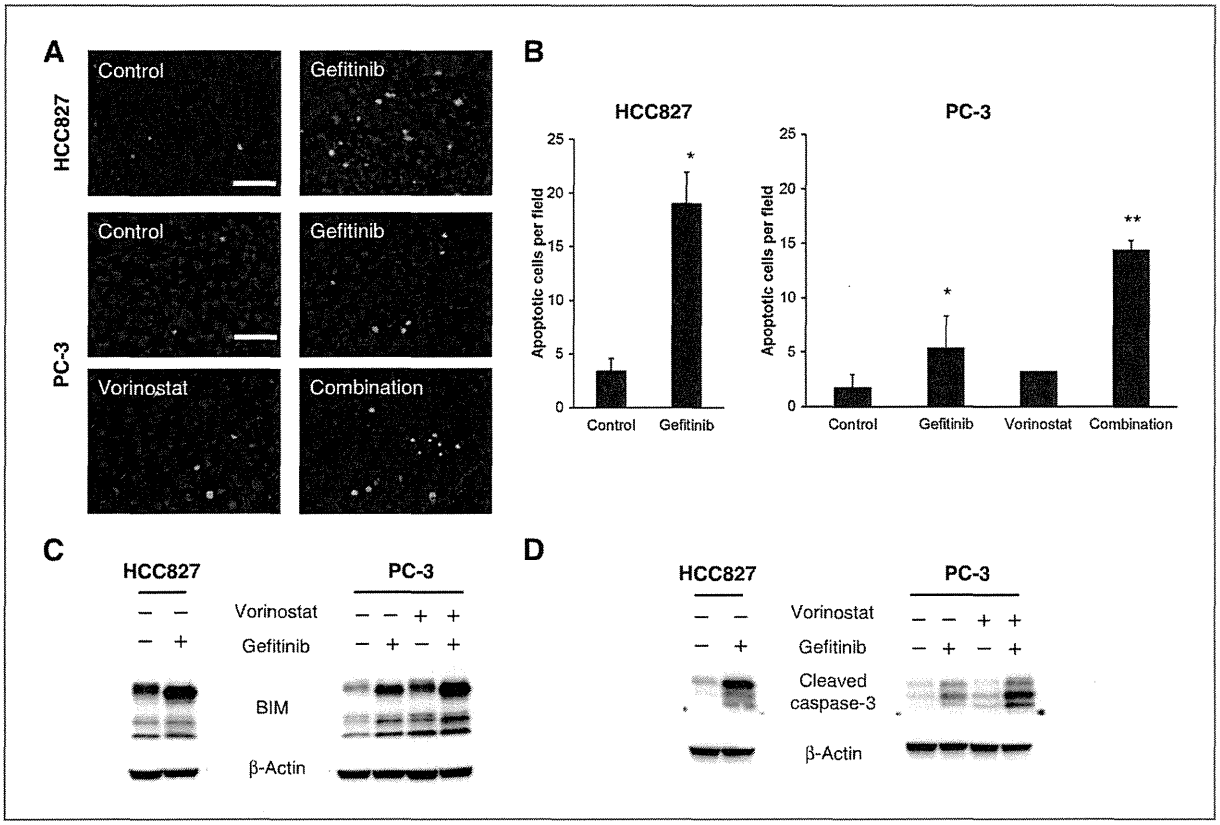

Figure 4. Vorinostat combined with gefitinib increases apoptosis in xenograft tumors with the *BIM* polymorphism. HCC827 and PC-3 xenograft tumors were resected from mice treated with 25 mg/kg gefitinib and/or 40mg/kg vorinostat for 4 days. A, analysis of apoptosis by TUNEL staining. Representative fluorescent images are shown. Green fluorescence indicates apoptotic cells. Bar indicates 50 μm. B, quantitation of number of apoptotic cells. *, $P < 0.05$ gefitinib or vorinostat versus control; **, $P < 0.05$ combination versus control and single agents. Bars represent mean ± SD. C, tumors were harvested 8 hours after 2 consecutive treatments with each compound, and the levels of protein in tumor lysates were determined by Western blotting. D, tumors were harvested 24 hours after 4 consecutive treatments with each compound. Protein expression levels in the tumor lysates were determined by Western blotting.

unselected patients with NSCLC, more than 65% of whom were Caucasian, failed to show therapeutic benefits (19). These findings suggest that the combination of vorinostat and an EGFR-TKI should be tested in selected patients with NSCLC with *EGFR* mutations and the *BIM* polymorphism.

Resistance to EGFR-TKIs associated with the *BIM* deletion polymorphism may be overcome by treatment with BH3 mimetics, such as ABT-737 (5). Although ABT-737 antagonized antiapoptotic proteins, such as Bcl-2 and Bcl-X_L, it did not antagonize the antiapoptotic protein Mcl-1, which is overexpressed in NSCLC (20), suggesting that the effects of BH3 mimetics may be limited to overcoming EGFR-TKI resistance caused by the *BIM* polymorphism in NSCLC. BH3 mimetics are being evaluated in early-phase clinical trials but are not ready for use in clinical practice. In contrast, vorinostat has been approved by the FDA for the treatment of patients with advanced primary cutaneous T-cell lymphoma (15). Therefore, the combination of gefitinib and vorinostat could easily be tested clinically.

The *BIM* polymorphism can be detected in formalin-fixed paraffin-embedded tumor tissues and peripheral blood (5). Moreover, a convenient and easy access PCR screening method can detect this polymorphism in circulating DNA from serum (Supplementary Fig. S5A and S5B). As the *BIM* polymorphism is a germline alteration, it can be assayed in serum obtained at any time point. Collectively, our findings illustrate the importance of clinical trials testing the ability of combinations of vorinostat and EGFR-TKIs to overcome EGFR-TKI resistance associated with the *BIM* polymorphism in patients with *EGFR*--mutant NSCLC.

Disclosure of Potential Conflicts of Interest

T. Nakagawa is an employee of Eisai Co., Ltd. for oncology research. Y. Hasegawa received research funding from Chugai Pharmaceutical Co., Ltd., Merck Sharp & Dohme Corp., AstraZeneca, and TAIHO Pharmaceutical Co., Ltd. S. Yano received honoraria from Chugai Pharmaceutical Co., Ltd. and AstraZeneca and received research funding from Chugai Pharmaceutical Co., Ltd., Kyowa Hakko Kirin Co., Ltd., and Eisai Co., Ltd. No potential conflicts of interest were disclosed by the other authors.

Authors' Contributions

Conception and design: T. Nakagawa, S. Takeuchi, S. Nanjo, S. Yano
Development of methodology: T. Nakagawa, S. Takeuchi
Acquisition of data (provided animals, acquired and managed patients, provided facilities, etc.): T. Nakagawa, D. Ishikawa, Y. Hasegawa

Published OnlineFirst February 4, 2013; DOI: 10.1158/0008-5472.CAN-12-3479

Analysis and interpretation of data (e.g., statistical analysis, biostatistics, computational analysis): T. Nakagawa, S. Yano
Writing, review, and/or revision of the manuscript: T. Nakagawa, S. Takeuchi, H. Ebi, M. Sato, Y. Hasegawa, Y. Sekido, S. Yano
Administrative, technical, or material support (i.e., reporting or organizing data, constructing databases): T. Yamada, T. Sano, M. Sato, Y. Sekido
Study supervision: S. Takeuchi, Y. Sekido, S. Yano

Acknowledgments

The authors thank Dr. John Minna (University of Texas Southwestern Medical Center) for the HCC2279 cells.

Grant Support

This study was supported by Grants-in-Aid for Cancer Research (21390256 to S. Yano; 11019957 to S. Takeuchi), Scientific Research on Innovative Areas "Integrative Research on Cancer Microenvironment Network" (22112010A01 to S. Yano), and Grant-in-Aid for Project for Development of Innovative Research on Cancer Therapeutics (P-Direct) from the Ministry of Education, Culture, Sports, Science, and Technology (MEXT) of Japan.

Received September 3, 2012; revised December 20, 2012; accepted January 19, 2013; published OnlineFirst February 4, 2013.

References

1. Maemondo M, Inoue A, Kobayashi K, Sugawara S, Oizumi S, Isobe H, et al.North-East Japan Study Group. Gefitinib or chemotherapy for non-small-cell lung cancer with mutated EGFR. N Engl J Med 2010;362:2380–8.
2. Pao W, Chmielecki J. Rational, biologically based treatment of EGFR-mutant non-small-cell lung cancer. Nat Rev Cancer 2010;10:760–74.
3. Sequist LV, Waltman BA, Dias-Santagata D, Digumarthy S, Turke AB, Fidias P, et al. Genotypic and histological evolution of lung cancers acquiring resistance to EGFR inhibitors. Sci Transl Med 2011; 3:75ra26.
4. Yano S, Wang W, Li Q, Matsumoto K, Sakurama H, Nakamura T, et al. Hepatocyte growth factor induces gefitinib resistance of lung adenocarcinoma with epidermal growth factor receptor-activating mutations. Cancer Res 2008;68:9479–87.
5. Ng KP, Hillmer AM, Chuah CT, Juan WC, Ko TK, Teo AS, et al. A common BIM deletion polymorphism mediates intrinsic resistance and inferior responses to tyrosine kinase inhibitors in cancer. Nat Med 2012;18:521–8.
6. O'Connor L, Strasser A, O'Reilly LA, Hausmann G, Adams JM, Cory S, et al. Bim: a novel member of the Bcl-2 family that promotes apoptosis. EMBO J 1998;17:384–95.
7. Chen L, Willis SN, Wei A, Smith BJ, Fletcher JI, Hinds MG, et al. Differential targeting of prosurvival Bcl-2 proteins by their BH3-only ligands allows complementary apoptotic function. Mol Cell 2005;17: 393–403.
8. Heath-Engel HM, Shore GC. Regulated targeting of Bax and Bak to intracellular membranes during apoptosis. Cell Death Differ 2006;13: 1277–80.
9. Costa DB, Halmos B, Kumar A, Schumer ST, Huberman MS, Boggon TJ, et al. BIM mediates EGFR tyrosine kinase inhibitor-induced apoptosis in lung cancers with oncogenic EGFR mutations. PLoS Med 2007;4:1669–79.
10. Fukazawa H, Noguchi K, Masumi A, Murakami Y, Uehara Y. BimEL is an important determinant for induction of anoikis sensitivity by mitogen-activated protein/extracellular signal-regulated kinase kinase inhibitors. Mol Cancer Ther 2004;3:1281–8.
11. Liu JW, Chandra D, Tang SH, Chopra D, Tang DG. Identification and characterization of Bimgamma, a novel proapoptotic BH3-only splice variant of Bim. Cancer Res 2002;62:2976–81.
12. Faber AC, Corcoran RB, Ebi H, Sequist LV, Waltman BA, Chung E, et al. BIM expression in treatment-naive cancers predicts responsiveness to kinase inhibitors. Cancer Discov 2011;1:352–65.
13. Bolden JE, Peart MJ, Johnstone RW. Anticancer activities of histone deacetylase inhibitors. Nat Rev Drug Discov 2006;5:769–84.
14. Mann BS, Johnson JR, Cohen MH, Justice R, Pazdur R. FDA approval summary: vorinostat for treatment of advanced primary cutaneous T-cell lymphoma. Oncologist 2007;12:1247–52.
15. Xargay-Torrent S, Lopez-Guerra M, Saborit-Villarroya I, Rosich L, Campo E, Roue G, et al. Vorinostat-induced apoptosis in mantle cell lymphoma is mediated by acetylation of proapoptotic BH3-only gene promoters. Clin Cancer Res 2011;17:3956–68.
16. Delcuve GP, Khan DH, Davie JR. Roles of histone deacetylases in epigenetic regulation: emerging paradigms from studies with inhibitors. Clin Epigenetics 2012;4:5.
17. Sharma SV, Lee DY, Li B, Quinlan MP, Takahashi F, Maheswaran S, et al. A chromatin-mediated reversible drug-tolerant state in cancer cell subpopulations. Cell 2010;141:69–80.
18. Witta SE, Gemmill RM, Hirsch FR, Coldren CD, Hedman K, Ravdel L, et al. Restoring E-cadherin expression increases sensitivity to epidermal growth factor receptor inhibitors in lung cancer cell lines. Cancer Res 2006;66:944–50.
19. Witta SE, Jotte RM, Konduri K, Neubauer MA, Spira AI, Ruxer RL, et al. Randomized phase II trial of erlotinib with and without entinostat in patients with advanced non-small-cell lung cancer who progressed on prior chemotherapy. J Clin Oncol 2012;30:2248–55.
20. Cetin Z, Ozbilim G, Erdogan A, Luleci G, Karauzum SB. Evaluation of PTEN and Mcl-1 expressions in NSCLC expressing wild-type or mutated EGFR. Med Oncol 2010;27:853–60.

The American Journal of Pathology, Vol. 182, No. 5, May 2013

ELSEVIER

The American Journal of
PATHOLOGY

ajp.amjpathol.org

TUMORIGENESIS AND NEOPLASTIC PROGRESSION

Surfactant Protein A Suppresses Lung Cancer Progression by Regulating the Polarization of Tumor-Associated Macrophages

Atsushi Mitsuhashi,* Hisatsugu Goto,* Takuya Kuramoto,* Sho Tabata,* Sawaka Yukishige,* Shinji Abe,* Masaki Hanibuchi,* Soji Kakiuchi,* Atsuro Saijo,* Yoshinori Aono,* Hisanori Uehara,† Seiji Yano,‡ Julie G. Ledford,§ Saburo Sone,* and Yasuhiko Nishioka*

From the Departments of Respiratory Medicine and Rheumatology and Molecular and Environmental Pathology,† Institute of Health Biosciences, The University of Tokushima Graduate School, Tokushima, Japan; the Division of Medical Oncology,‡ Cancer Research Institute, Kanazawa University, Kanazawa, Japan; and the Division of Pulmonary, Allergy, and Critical Care Medicine,§ Duke University Medical Center, Durham, North Carolina*

Accepted for publication January 10, 2013.

Address correspondence to Yasuhiko Nishioka, M.D., Ph.D., Department of Respiratory Medicine and Rheumatology, Institute of Health Biosciences, The University of Tokushima Graduate School, 3-18-15 Kuramoto-cho Tokushima, 770-8503, Japan. E-mail: yasuhiko@clin.med.tokushima-u.ac.jp.

Surfactant protein A (SP-A) is a large multimeric protein found in the lungs. In addition to its immunoregulatory function in infectious respiratory diseases, SP-A is also used as a marker of lung adenocarcinoma. Despite the finding that SP-A expression levels in cancer cells has a relationship with patient prognosis, the function of SP-A in lung cancer progression is unknown. We investigated the role of SP-A in lung cancer progression by introducing the SP-A gene into human lung adenocarcinoma cell lines. SP-A gene transduction suppressed the progression of tumor in subcutaneous xenograft or lung metastasis mouse models. Immunohistochemical analysis showed that the number of M1 antitumor tumor-associated macrophages (TAMs) was increased and the number of M2 tumor-promoting TAMs was not changed in the tumor tissue produced by SP-A–expressing cells. In addition, natural killer (NK) cells were also increased and activated in the SP-A–expressing tumor. Moreover, SP-A did not inhibit tumor progression in mice depleted of NK cells. Taking into account that SP-A did not directly activate NK cells, these results suggest that SP-A inhibited lung cancer progression by recruiting and activating NK cells via controlling the polarization of TAMs. *(Am J Pathol 2013, 182: 1843–1853; http://dx.doi.org/10.1016/j.ajpath.2013.01.030)*

Lung cancer is the major cause of malignancy-related death worldwide. Mortality is 80% to 90%, which makes this disease the leading cause of cancer-related deaths.[1] The high mortality rate of this disease is primarily due to the difficulty of early diagnosis, the high metastatic potential, and the poor responses to chemical therapy and radiotherapy. Because there is no established curative therapy for advanced lung cancer to date, clinical management is palliative in many cases. Therefore, it is crucial to investigate and understand the underlying biological and molecular mechanisms of lung cancer progression.

Surfactant protein A (SP-A) is a large multimeric protein found in the airways and alveoli of the lungs. SP-A is a member of the collectin family of proteins, characterized by NH_2-terminal collagen-like regions and COOH-terminal lectin domains. Although other SPs, such as SP-B, function to reduce surface tension in the lungs, SP-A (and SP-D) regulates the pulmonary immune response.[2] Previous *in vivo* studies have shown that SP-A regulates responses involved in initiation and potentiation of inflammation by regulating the production of proinflammatory cytokines, such as tumor necrosis factor α (TNF-α), in response to lipopolysaccharide[3] or by accelerating the clearance of a variety of pathogens.[4–8] Because SP-A has the ability to opsonize and enhance pathogen uptake by phagocytes, the immunoregulatory roles of SP-A have been studied mainly in the field of infectious diseases. Recently, we reported that

Supported by the Ministry of Education, Culture, Sports, Science and Technology Grants-in Aid for Scientific Research (MEXT KAKENHI) grant 22790759 (H.G.) and NIH grants AI-81672 and HL-111151 (J.G.L.).

A.M. and H.G. contributed equally to this work.

http://dx.doi.org/10.1016/j.ajpath.2013.01.030

SP-A has a role in regulating bleomycin-induced acute noninfectious lung injury by inhibiting lung epithelial cell apoptosis.[9] Pastva et al[10] reported that SP-A regulates T_H2 cytokine production in a mouse asthma model. These results suggest that SP-A has diverse functions to control various lung diseases. Considering that SP-A contributes to multiple aspects of pulmonary host defense, we hypothesized that SP-A might have a role in lung cancer progression.

In a lung cancer study, SP-A was expressed in approximately 49% of primary non–small cell lung carcinomas[11] and is used as a specific marker of carcinoma that originates in type II pneumocytes. In addition, a previous study demonstrated that deletion of the *SFTPA1* (alias, *SPA*) gene in non–small cell lung cancer cells was associated with tumor progression.[12] Tsutsumida et al[13] found that patients with lung adenocarcinoma with relatively high MUC1 mucin expression and low SP-A expression in cancer cells had a poor outcome. These clinical studies demonstrate that in addition to use as a diagnostic marker, SP-A expression in lung cancer cells could be a useful biomarker of good prognosis. Although these studies suggested that SP-A might have a role in suppressing lung cancer progression, the role of SP-A in lung cancer has not been extensively studied, and the mechanisms by which SP-A controls lung cancer progression remain unknown.

In this study, we generated SP-A–overexpressing human lung adenocarcinoma cells and evaluated the role of SP-A in lung cancer progression using experimental mouse models.

Materials and Methods

Cell Lines

The human lung adenocarcinoma cell line PC14PE6 was a gift from Dr. Isaiah J. Fidler (The University of Texas MD Anderson Cancer Center, Houston TX). The human lung adenocarcinoma cell line A549 was purchased from ATCC (Manassas, VA). These cell lines were authenticated by BEX Co. Ltd. (Tokyo, Japan) using a multiplex short tandem repeat assay. Both cell lines were maintained in RPMI 1640 medium supplemented with 10% heat-inactivated fetal bovine serum, 100 U/mL of penicillin, and 50 μg/mL of streptomycin and were cultured at 37°C in a humidified atmosphere of 5% CO_2 in air.

Reagents

An anti-mouse IL-2 receptor β-chain monoclonal antibody, TM-β1 (IgG2b), was a gift from Drs. Masayuki Miyasaka and Toshio Tanaka (Osaka University, Osaka, Japan).

SP-A Purification

SP-A was purified from the lung lavage fluid of patients with alveolar proteinosis as previously described[14] and was routinely tested to reduce endotoxin contamination.[14] Briefly, SP-A was suspended in 100 mmol/L octylglucoside and 5 mmol/L Tris, pH 7.4, after butanol extraction.

Table 1 Primer Sequences Used in Quantitative PCR

	Forward	Reverse	Product size (bp)
Gene (mouse)			
IL-1β	5′-TGACGTTCCCATTAGACAAC-3′	5′-ATTTTGTCGTTGCTTGGTTC-3′	171
IL-6	5′-GTACCATAGCTACCTGGAGT-3′	5′-GGAAATTGGGGTAGGAAGGA-3′	154
TNF-α	5′-CCTATGTCTCAGCCTCTTCT-3′	5′-TTGGGAACTTCTCATCCCTT-3′	107
IL-12	5′-CACACTGGACCAAAGGGACT-3′	5′-TGGTTTGATGATGTCCCTGA-3′	169
IFN-γ	5′-TAGCTCTGAGACAATGAACG-3′	5′-CACATCTATGCCACTTGAGT-3′	145
CCL2	5′-TTCACAGTTGCCGGCTGG-3′	5′-TGAATGAGTAGCAGCAGGTGAGTG-3′	81
CCL5	5′-CAGCAGCAAGTGCTCCAATCTT-3′	5′-TTCTTGAACCCACTTCTTCTCTGG-3′	91
IL-10	5′-AAGGACCAGCTGGACAACAT-3′	5′-TCTCACCCAGGGAATTCAAA-3′	172
MRC-1	5′-TGCAAGGATCATACTTCCCT-3′	5′-TGATGTTCTCCAGTAGCCAT-3′	240
Arg1	5′-GAATGGAAGAGTCAGTGTGG-3′	5′-AATGACACATAGGTCAGGGT-3′	97
CD163	5′-GACGACAGATTCAGCGACTT-3′	5′-CCGAGGATTTCAGCAAGTCCA-3′	114
Prf1	5′-GACACAGTAGAGTGTCGCAT-3′	5′-TTTTGAAGTCAAGGTGGAGTG-3′	70
GzmB	5′-AGAGAGCAAGGACAACACTC-3′	5′-ATCGAAAGTAAGGCCATGTAG-3′	176
B2M (β_2M)	5′-GGAAGCCGAACATACTGAACTG-3′	5′-TTTCCCGTTCTTCAGCATTTGG-3′	80
Gene (human)			
IL-1β	5′-GACAGGATATGGAGCAACAA-3′	5′-GCTGTAGAGTGGGCTTATCA-3′	147
IL-6	5′-CCTCTTCAGAACGAATTGAC-3′	5′-AGTCTCCTCATTGAATCCAG-3′	186
TNF-α	5′-GGCAGTCAGATCATCTTCTCG-3′	5′-CAGCTGGTTATCTCTCAGCTC-3′	148
CCL2	5′-CTCATAGCAGCCACCTTCATT-3′	5′-ACAGATCTCCTTGGCCACAA-3′	192
CCL3	5′-GGCAGTCAGATCATCTTCTCG-3′	5′-CAGCTGGTTATCTCTCAGCTC-3′	81
CCL5	5′-CTGTCATCCTCATTGCTACTG-3′	5′-GCCACTGGTGTAGAAATACTC-3′	140
MRC-1	5′-CCATCGAGGAATTGGACTTT-3′	5′-TGTCATTTAAGCCGATCCAC-3′	78
RPL27	5′-ATCGCCAAGAGATCAAAGATAA-3′	5′-TCTGAAGACATCCTTATTGACG-3′	123

Polymyxin-agarose (Sigma-Aldrich, St. Louis, MO) was added 1:5 (v/v) and allowed to incubate at room temperature for 30 minutes. The mixture was then dialyzed (14,000 molecular weight cutoff value) for four changes ≥4 hours each against autoclaved 5 mmol/L Tris, pH 7.4. The mixture was then centrifuged, and the supernatant, containing SP-A, was removed by gentle aspiration. SP-A preparations had final endotoxin concentrations of <0.1 pg/μg of SP-A as determined by the Limulus amoebocyte lysate assay (QCL-1000; BioWhittaker, Walkersville, MD).

SPA Gene Transduction

The human *SPA* gene—expressed region [SFTPA1 (NM_005411)] (OriGene Technologies, Rockville, MD) was introduced into the pMIG vector (a gift from Dr. Alana L. Welm, University of Utah, Salt Lake City). The Platinum-E packaging cell line (a gift from Dr. Toshio Kitamura, Tokyo University, Tokyo, Japan)[15] was transfected with pMIG or derivative vector DNA by using FuGENE 6 transfection reagent (Roche Applied Science, Indianapolis, IN). PC14PE6 or A549 cells were infected using the viral supernatant as described previously.[16] The proportion of green fluorescent protein—positive cells was >90% in the entire population.

Animals

Male athymic BALB/c nude mice and SCID mice were obtained from Charles River Laboratories Japan (Yokohama) and CLEA Japan (Tokyo), respectively, and were maintained under specific pathogen-free conditions throughout the study. All the experiments were performed in accordance with the guidelines established by The University of Tokushima Committee on Animal Care and Use, Tokushima, Japan. At the end of each *in vivo* experiment, the mice were anesthetized with isoflurane and euthanized humanely by cutting the subclavian artery. All the experiment protocols were reviewed and approved by the Animal Research Committee of The University of Tokushima.

In Vivo Subcutaneous Xenograft Model

PC14PE6 cells (1.0×10^6 per mouse) or A549 cells (3.0×10^6 per mouse) suspended in 0.1 mL of PBS were subcutaneously inoculated into the right flank of nude mice. Tumor size was measured using a vernier caliper three times a week (volume = $ab^2/2$, where a indicates long diameter; b, short diameter). The mice were euthanized humanely on day 21, and the tumors were resected for further analyses.

In Vivo Lung Metastasis Model

To establish lung metastasis, nude mice were intravenously inoculated via the tail vein with 1.0×10^6 tumor cells per mouse.[17] The mice were euthanized humanely on either day 28 (PC14PE6) or day 42 (A549). The lungs were weighed, and the number of metastatic colonies on the surface of the lungs was determined by visual examination. Because PC14PE6 cells produce large amounts of pleural effusion,[18] the volume of the effusion was also evaluated. In some experiments, natural killer (NK) cells were depleted by treating nude mice with TM-β1 5 days after inoculation of PC14PE6 cells.[19]

Immunofluorescence

The excised tumor tissue was placed into OCT compound (Sakura Finetechnical Co., Tokyo, Japan) and snap frozen. Eight-micrometer-thick frozen tissue sections were fixed with 4% paraformaldehyde solution in PBS and were used for identification of macrophages using 1:150 rat anti-mouse CD68 monoclonal antibody (Serotec, Oxford, UK) and of NK cells using 1:100 goat anti-mouse NKp46/NCR1 monoclonal antibody (R&D Systems, Minneapolis, MN). Alexa Fluor 488—labeled secondary antibodies (dilution 1:250; Invitrogen, Carlsbad, CA) were used for immunofluorescence (IF) detection. To identify M1 or M2 macrophages, the sections were stained with 1:150 fluorescein isothiocyanate—conjugated rat anti-mouse TNF-α antibody (BD Pharmingen, Franklin Lakes, NJ) or 1:150 fluorescein isothiocyanate—conjugated rat anti-mouse CD206 [mannose

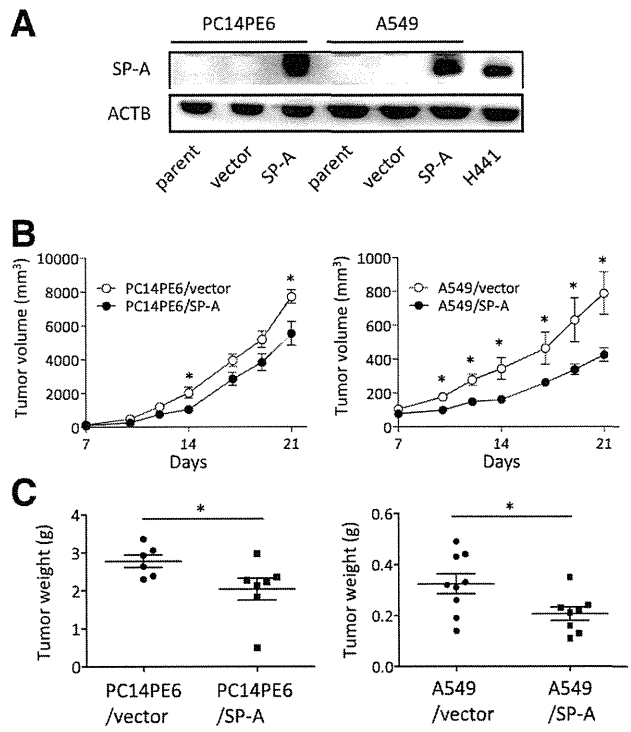

Figure 1 The effect of SP-A on lung cancer subcutaneous xenografts *in vivo*. **A:** SP-A expression of human SP-A stable transfectants was confirmed by Western blot analysis. H441 cells were used as a positive control. ACTB, β-actin. Tumor growth (**B**) and weight (**C**) of xenografts produced by PC14PE6 (**left panels**; $n = 6$ per group) and A549 (**right panels**; $n = 8$ per group) cells transduced with SP-A or vector. Data are presented as means ± SEM (**horizontal lines** in **C**). $^*P < 0.05$.

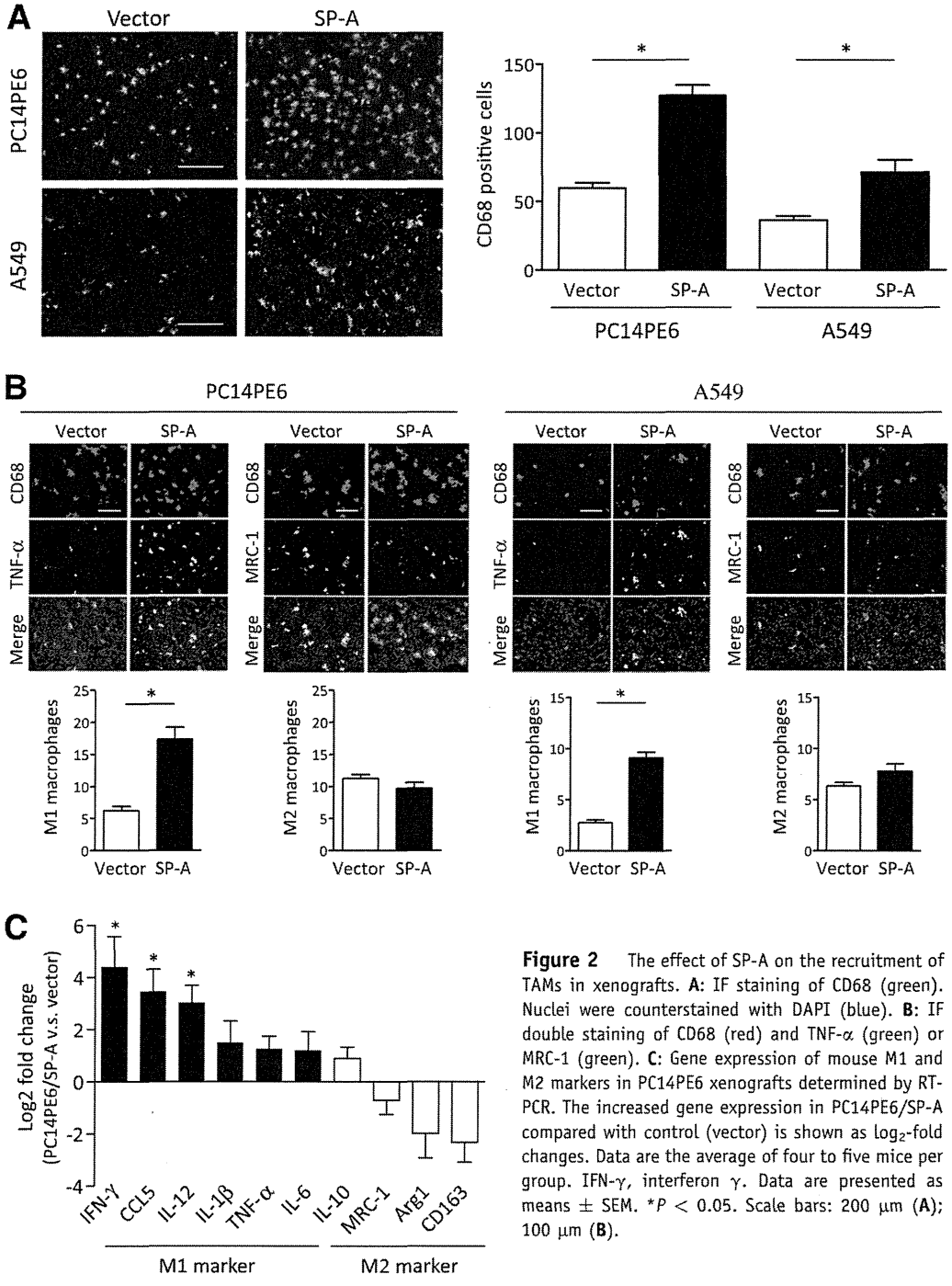

Figure 2 The effect of SP-A on the recruitment of TAMs in xenografts. **A**: IF staining of CD68 (green). Nuclei were counterstained with DAPI (blue). **B**: IF double staining of CD68 (red) and TNF-α (green) or MRC-1 (green). **C**: Gene expression of mouse M1 and M2 markers in PC14PE6 xenografts determined by RT-PCR. The increased gene expression in PC14PE6/SP-A compared with control (vector) is shown as $\log_2$-fold changes. Data are the average of four to five mice per group. IFN-γ, interferon γ. Data are presented as means ± SEM. $^*P < 0.05$. Scale bars: 200 μm (**A**); 100 μm (**B**).

receptor C type 1 (MRC-1)] antibody (BioLegend, San Diego, CA) after CD68 staining. Alexa Fluor 594–labeled anti-rat secondary antibodies (dilution 1:250; Invitrogen) were used for CD68 IF detection. M1 or M2 macrophages were identified as CD68-positive/TNF-α-–positive or CD68-positive/MRC-1–positive cells, respectively. Nuclei were counterstained with DAPI (blue). In each slide, the number of positive cells was counted in five areas under fluorescent microscopy at ×100 (single staining) or ×200 (double staining) magnification.

RT-qPCR

Total RNA was extracted from the tumors using the RNeasy mini kit (Qiagen, Valencia, CA) and reverse transcribed to cDNA using a high-capacity cDNA Reverse Transcription kit (Applied Biosystems, Carlsbad, CA) according to the manufacturer's instructions. RT-PCR was performed using the CFX96 real-time PCR system (Bio-Rad Laboratories, Hercules, CA) using SYBR Premix Ex Taq (Takara, Kyoto, Japan). Human RPL27[20] and mouse β2m mRNA were used

as housekeeping genes, and quantification was determined by using the $\Delta\Delta C_T$ method. Specific PCR primer pairs for each studied gene are shown in Table 1.

SP-A Stimulation of Monocytes, Macrophages, and NK Cells

Human monocytes were separated from the peripheral blood of healthy volunteers as described previously.[21] The purity and viability of the monocytes was confirmed to be >98% by staining with Diff-Quik (Baxter Diagnostics, Deerfield, IL) and trypan blue, respectively. Mouse alveolar macrophages (AMs) were collected by using bronchoalveolar lavage as described previously.[9] More than 95% of the cells were confirmed to be AMs. For eliciting mouse peritoneal macrophages (PMs), 2 mL of thioglycollate (BD Biosciences, San Jose, CA) was injected into the peritoneal cavity of SCID mice. After 3 days, peritoneal exudative cells were harvested by intraperitoneal lavage with ice-cold PBS. Approximately 80% of isolated cells were macrophages. NK cells from SCID mice were isolated as previously described.[22] These immune cells were stimulated with 20 μg/mL of human SP-A for 4 hours in RPMI 1640 medium containing 1% fetal bovine serum. Total RNA was extracted for quantitative RT-PCR.

Cell Migration Assay

The migration assay was performed using 8-μm pore size cell culture inserts (BD Biosciences). After 24 hours of serum starvation, PMs in serum-free media were added to the inner chamber in the presence or absence of 20 μg/mL of SP-A. RPMI 1640 medium containing 10% fetal bovine serum was added to the lower chamber. After 17 hours of incubation, the cells that had migrated to the bottom surface of the filter were counted in six randomly selected fields on each filter under a microscope at ×200 magnification.

Western Blot Analysis

Twenty micrograms of total protein extracted from tumor cell lines was resolved by SDS-PAGE (Invitrogen) and was transferred to polyvinylidene difluoride membrane (Atto Corp., Tokyo, Japan), and Western blot was performed as described previously.[9] Immunoreactive bands were visualized using SuperSignal west femto maximum sensitivity substrate (Thermo Scientific, Waltham, MA).

Statistical Analysis

Data are given as means ± SEM. Statistical analysis was performed using the Student's *t*-test of unpaired samples or the *U*-test. Values of $P < 0.05$ were considered statistically significant.

Results

Effect of SP-A on Lung Cancer Xenografts *in Vivo*

Human lung adenocarcinoma cell lines (PC14PE6 and A549 cells) were transduced with vectors encoding human SP-A by the retroviral transduction system (termed PC14PE6/SP-A and A549/SP-A, respectively). The empty vector was transduced as a control (termed PC14PE6/vector and A549/vector, respectively) (Figure 1A). To investigate the effect of SP-A on *in vivo* tumor growth, we initially injected male nude mice subcutaneously with these cells. For both cell lines, the growth of xenografts was significantly inhibited when cells were overexpressing SP-A compared with the vector control cells (Figure 1, B and C).

Direct Effect of SP-A on Lung Cancer Cell Proliferation

To explore the underlying mechanism by which SP-A suppressed the growth of xenografts, we performed immunohistochemical staining of Ki-67, CD31, or TUNEL (Supplemental Figure S1A). The number of Ki-67–positive cells was significantly decreased in tumors formed by SP-A overexpressing PC14PE6 cells, whereas no difference was seen in A549 cells. The number of TUNEL-positive cells was increased in both cell lines expressing SP-A. No difference was seen in the number of CD31-positive cells. These results led us to consider that SP-A might have a direct effect on cancer cell proliferation or the cell

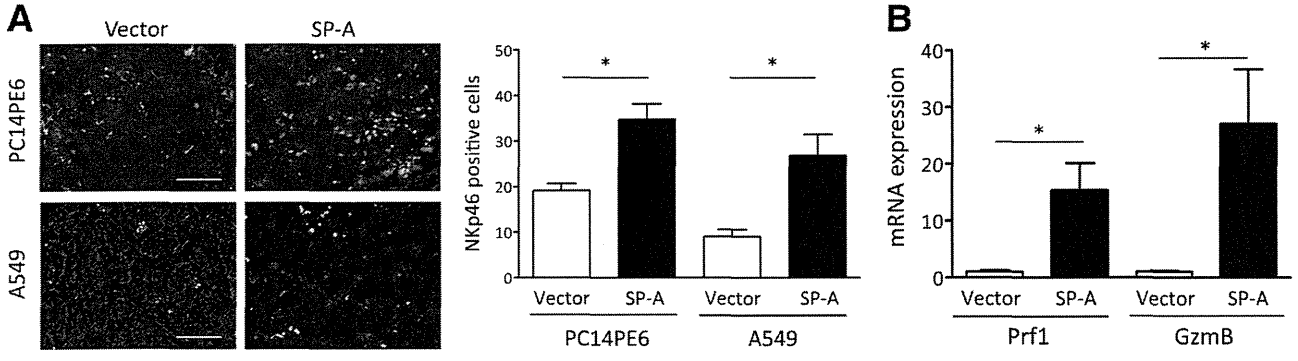

Figure 3 The effect of SP-A on NK cell recruitment in xenografts. **A:** IF staining of NKp46 (green). Nuclei were counterstained with DAPI (blue). Scale bars: 200 μm. **B:** Gene expression of mouse Prf1 and GzmB in PC14PE6 xenografts determined by RT-PCR. Data are the average of four to five mice per group. Data are presented as means ± SEM. *$P < 0.05$.

cycle. However, results of the *in vitro* MTT assay showed that SP-A–overexpressing cells had the same ability of cell proliferation with control cells in PC14PE6 and A549 cells (Supplemental Figure S1B). Propidium iodide staining revealed that the state of cell cycle and death was also similar by SP-A transduction in PC14PE6 cells (Supplemental Figure S1C). Moreover, the effect of SP-A on the cell cycle in PC14PE6 cells was also investigated by using the fluorescent ubiquitination-based cell-cycle indicator system, but no difference was observed (data not shown). Taken together, we considered that although SP-A inhibited tumor growth *in vivo*, its effect was not due to the direct effect on cell proliferation or the cell cycle or to the inhibition of tumor angiogenesis.

Effect of SP-A on the Recruitment of Tumor-Associated Macrophages

We next investigated whether cancer cell–produced SP-A might affect the tumor microenvironment. A variety of studies have shown that tumor-infiltrated tumor-associated macrophages (TAMs) play an important role in the progression of various types of cancers, including lung cancer.[23,24] It is also known that activated macrophages are functionally polarized into either M1 (classically activated) or M2 (alternatively activated) macrophages. M1 macrophages produce large amounts of inflammatory cytokines, such as TNF-α and interferon-γ, and are essential for tumor suppression and host defense against bacteria.[25] In contrast, M2 macrophages play important roles in tumor progression, tissue remodeling, and angiogenesis. M2 macrophages are characterized by their high expression of several factors, such as arginase-1, MRC-1, and IL-10. To determine whether SP-A affects the recruitment of TAMs, sections from resected tumors were subjected to IF staining. As shown in Figure 2A, the number of CD68-positive macrophages was significantly increased in tumors formed by SP-A–transduced cells. We then assessed whether M1 and M2 macrophage polarizations were altered by SP-A transduction. We performed IF double staining of CD68 and TNF-α for M1 and MRC-1 for M2 and determined M1 and M2 macrophages in the xenografts. In both SP-A–transduced cell lines, the number of M1 macrophages was significantly increased versus vector controls, whereas the number of M2 macrophages was not changed (Figure 2B). To confirm that the number of M1 macrophages was increased in the SP-A–expressing tumors, mRNA was extracted from the resected tumor, and the expression of M1 and M2 markers was determined by RT-PCR using mouse-specific primers. Multiple M1 markers were up-regulated in the SP-A–expressing tumors, whereas M2 markers were not changed compared with the vector control tumors (Figure 2C).

Effect of SP-A on NK Cell Recruitment in Xenografts

We next focused on the other important immune cells, NK cells. Because cytokines/chemokines such as interferon-γ, CCL5, and IL-12 that were up-regulated in the SP-A–expressing tumors are known to be potent inducers of NK cells,[26,27] we hypothesized that the *in vivo* tumor regression could be due to the recruitment of NK cells. Thus, we performed IF staining of NKp46 to determine the number of NK cells in the xenografts. As shown in Figure 3A, the number of

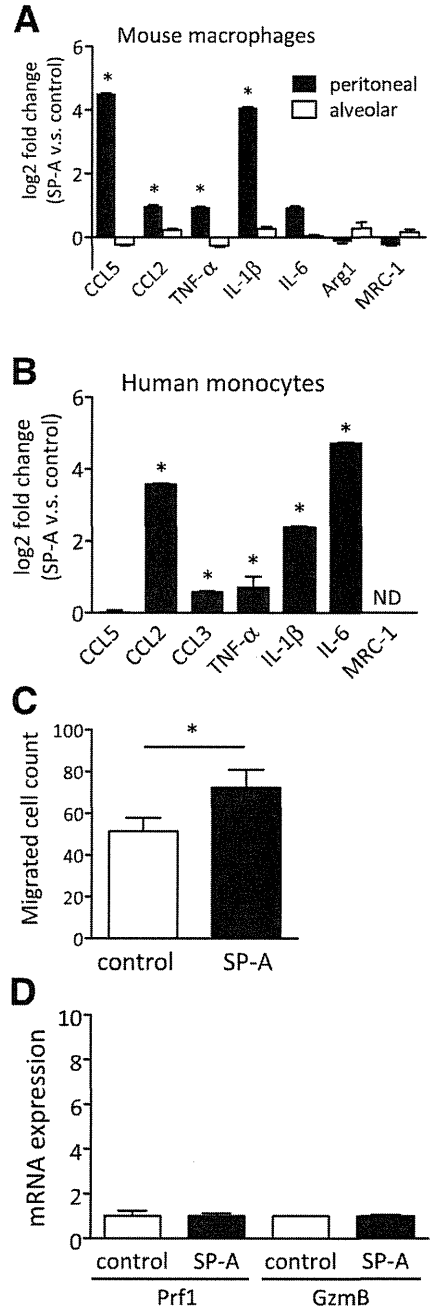

Figure 4 The effect of SP-A on various immune cells *in vitro*. After exogenous SP-A treatment, the expression of various genes was determined by RT-PCR in mouse PMs and AMs (**A**) and human peripheral monocytes (**B**). The increased gene expression in SP-A treatment compared with control (PBS) are shown as $\log_2$-fold changes (n = 3 per group). ND, not detected. **C**: The effect of exogenous SP-A on the migration of mouse PMs (n = 3 per group). **D**: Gene expressions of Prf1 and GzmB in mouse NK cells treated with exogenous SP-A (n = 3 per group). Data are presented as means ± SEM. *$P < 0.05$.